Non-Proprietary

Fluidic Device Design for the APR1400

APR1400-Z-M-TR-12003-NP-A

April 2017

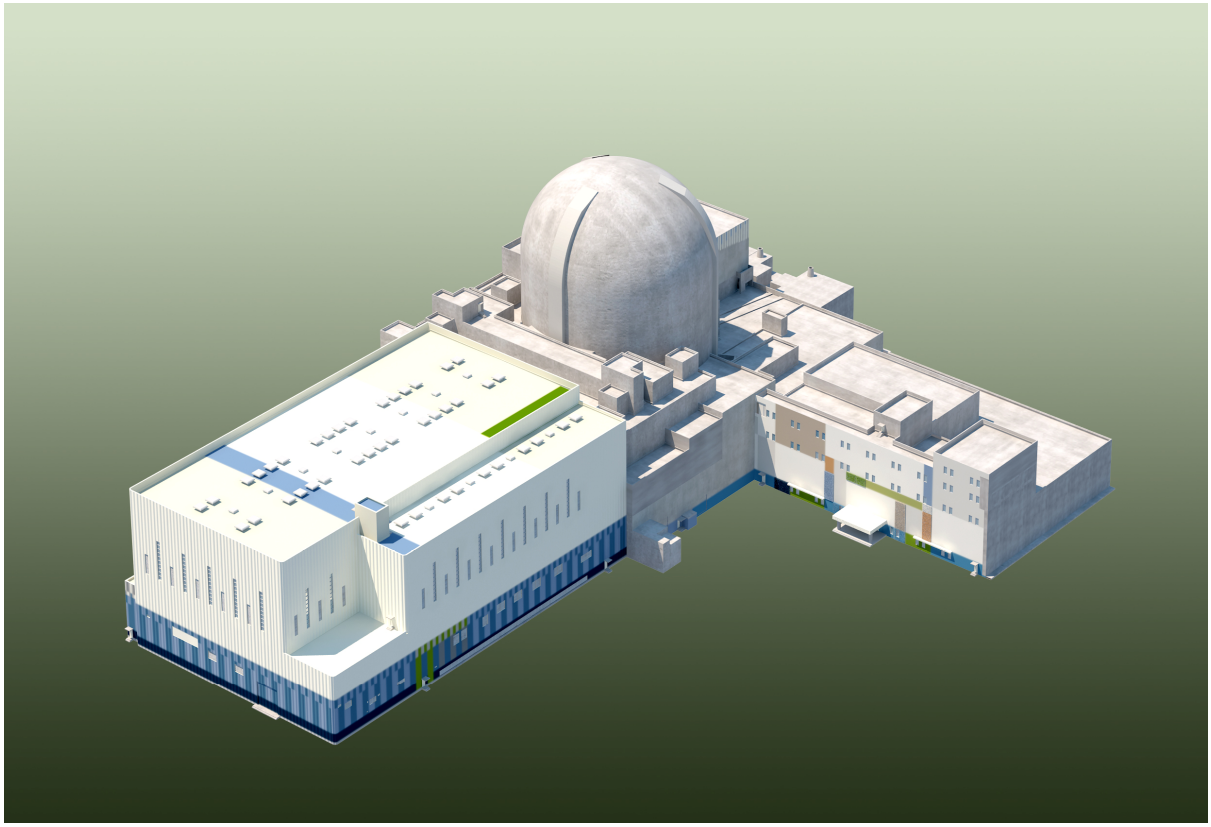

KOREA ELECTRIC POWER CORPORATION

KOREA HYDRO & NUCLEAR POWER CO., LTD

CONTENTS

SECTION A

Page intentionally left blank

Non-Proprietary

April 4, 2017

Dr. Han-Gon Kim, Project Manager
APR1400 Design Certification
Advanced Reactors Development Laboratory
Korea Hydro and Nuclear Power Co., Ltd.
70-1312-gil, Yuseong-daero
Yuseong-Gu, Daejeon
305-343 Korea (Republic of)

SUBJECT: ADVANCED POWER REACTOR 1400 FINAL SAFETY EVALUATION FOR TOPICAL REPORT APR1400-Z-M-TR-12003-P, REVISION 0, "FLUIDIC DEVICE DESIGN FOR THE APR1400"

Dear Dr. Kim:

The U.S. Nuclear Regulatory Commission (NRC) staff has prepared a final Topical Report Safety Evaluation (TRSE) for Topical Report APR1400-Z-M-TR12003-P, Revision 0, "Fluidic Device Design for the APR1400." This TRSE is also valid for the non-proprietary version of the topical report. This action is supported by the letter dated February 23, 2017 (ADAMS Accession No. ML17088A115), whereby the Advisory Committee on Reactor Safeguards agrees with the NRC staff's conclusions, within the limits and conditions that are specified in the TRSE. This evaluation is in support of the review of the APR1400 design certification application submitted by Korea Hydro and Nuclear Power (KHNP) and Korea Electric Power Corporation on December 23, 2014.

The staff requests that KHNP publish the accepted proprietary and non-proprietary versions of this topical report within one month of receipt of this letter. The accepted versions shall incorporate this letter and the enclosed final TRSE after the title page. Also, they must contain historical review information, including NRC requests for additional information and your responses. The accepted versions of the topical report shall include an "-A" (designated accepted) following the report identification number.

If the NRC's criteria or regulations change such that its conclusion that the accepted topical report is invalidated, KHNP and/or the applicant referencing the topical report will be expected either to revise and resubmit its respective documentation or to submit justification for continued applicability of the topical report without revision of the respective documentation.

If you have any questions or comments concerning this matter, please contact me at (301) 415–6391, or via e-mail at Jeff.Ciocco@nrc.gov, or Jessica Umana at (301) 415–5207, or via e-mail at Jessica.Umana@nrc.gov.

Sincerely,

/RA/

Jeffrey A. Ciocco, Senior Project Manager
Licensing Branch 2
Division of New Reactor Licensing
Office of New Reactors

Docket No. 52-046

Enclosure:
As stated

cc w/ encl.: See next page

SUBJECT: ADVANCED POWER REACTOR 1400 FINAL SAFETY EVALUATION FOR TOPICAL REPORT APR1400-Z-M-TR-12003-P, REVISION 0, "FLUIDIC DEVICE DESIGN FOR THE APR1400" DATE: April 4, 2017

DISTRIBUTION:

D101	RidsNroLaCSmith	RidsOgcMailCenter Resource
Public	RidsNroOd	RidsAcrsAcnwMailCTR Resource
LB2 R/F	GWunder, NRO	SVrahoretis, OGC
RidsNroDnrl	JCiocco, NRO	RidsNroDnrlLb2
MThomas, DSRA	JMonninger, NRO	RKaras, NRO

ADAMS Accession Nos.
Package – ML17088A109
Letter – ML17088A116
TSER – ML17088A115 ***via e-mail** **NRO-002**

OFFICE	DNRL/LB2: PM	DNRL: LA	DNRL/LB2: PM
NAME	JUmana	CSmith*	JCiocco
DATE	04/03/2017	04/03/2017	04/04/ 2017

OFFICIAL RECORD COPY

KHNP Mailing List

9/22/2015

Daegeun Tony Ahn
Director
KHNP Washington DC Center
8100 Boone Blvd, Suite 620
Vienna, VA 22182

Email

kimhg1108@khnp.co.kr [Han-Gon Kim]
hansang.kim@khnp.co.kr [Hansang Kim]
dohwan.lee@khnp.co.kr [Do-Hwan Lee]
junghokim@khnp.co.kr [Jung-Ho Kim]
yunho.kim@khnp.co.kr [Yun Ho Kim]
jiyong.oh@khnp.co.kr [Jiyong Andy Oh]
ahn.daegeun@khnp.co.kr, [Daegeun Tony Ahn]
jksuh@khnp.co.kr [Jeong Kwan Suh]
hachewung@khnp.co.kr [Che Wung Ha]
kang.deogji@khnp.co.kr [Deog Ji Kang]
sunguk.kwon@khnp.co.kr [Sun Guk Kwon]
ptmaster300@kepco.co.kr [Hyun Chul Park]

Non-Proprietary

TOPICAL REPORT SAFETY EVALUATION (TRSE)

BY THE OFFICE OF NEW REACTORS OF

TOPICAL REPORT APR1400-Z-M-TR-12003-P, REVISION 0,

"FLUIDIC DEVICE DESIGN FOR THE APR1400"

KOREA HYDRO & NUCLEAR POWER CO., LTD.

PROJECT NO. PROJ0782

CONTENTS

1.0 INTRODUCTION

In support of the application for the design certification for the Advanced Power Reactor 1400 (APR1400), Korea Hydro & Nuclear Power Co., Ltd., hereinafter referred to as the applicant, submitted Topical Report APR1400-Z-M-TR-12003-P, Revision 0, “Fluidic Device Design for the APR1400” (Reference 1). The APR1400 design uses pressurized safety injection tanks (SITs) installed with passive, flow controlling fluidic devices (FD) as a part of the emergency core cooling system (ECCS) design, otherwise referred to as the safety injection system (SIS). The APR1400 SIT with FD (SIT-FD) is designed on the operating experience of a conventional accumulator used for mitigating the consequences of loss-of-coolant accidents (LOCAs) in pressurized water reactors (PWRs). Similar to the conventional accumulators used in the operating PWR plants, the SIT is an accumulator tank partially filled with borated water and pressurized with nitrogen. The APR1400 SIT design differs from the conventional accumulators in that it incorporates a flow controlling FD at the exit of the tank to provide a means for passive flow control. The SIT is attached to the primary system through a series of check valves and an isolation valve, and is aligned during normal plant operation to allow flow into the primary coolant system if the primary system pressure drops below the pressure setpoint of the SIT. The flow controlling FD can provide an extended injection flow rate without the need for any moving parts.

Emergency core cooling (ECC) during a LOCA is one of the primary functions of the ECCS. In a conventional nuclear plant, the ECCS consists of accumulators, the high-head SIS, and the low-head SIS to accomplish the ECC functions. During a large break LOCA (LBLOCA), the fuel cladding temperature increases due to the lack of liquid around the core. A LBLOCA generally includes blowdown, refill, reflood, and long-term cooling phases. After the initial blowdown, the ECCS is required to inject water into the core to limit the rise of fuel temperature in three steps. In the refill phase, the accumulators quickly inject water at a high flow rate to fill the lower plenum and downcomer of the reactor vessel. Subsequently, the core is reflooded by the water head in the downcomer, and the high-head SIS and low-head SIS inject flow to keep high water level in the downcomer to maintain reflooding of the core. In the long-term cooling phase after core reflood is completed, the low-head SIS provides water to remove decay heat and maintain the core in a flooded state.

In the APR1400 SIS design, the SIT switches its flow rate from large-flow injection to small-flow injection automatically and passively after the water level in the tank drops below the top of the standpipe. During a LBLOCA, it is necessary to start the SIS pumps prior to the end of accumulator injection. The SIT injects water for a longer period of time than a conventional accumulator, thereby allowing more time to start the SIS pumps.

Topical Report APR1400-Z-M-TR-12003-P, Revision 0, “Fluidic Device Design for the APR1400,” (Reference 1) describes the SIT-FD design, the principles of operation and important design features of SIT-FD, as well as full scale experiments confirming the performance of the SIT-FD.

2.0 REGULATORY BASIS

The staff's review of APR1400-Z-M-TR-12003-P, Revision 0, is based on conformance with the following regulatory requirements:

General Design Criterion (GDC) 35, "Emergency Core Cooling," in Appendix A to Title 10 of the *Code of Federal Regulations* (10 CFR) as it relates to the requirement of a system that would provide abundant ECC to satisfy the ECCS safety function of transferring heat from the reactor core following any loss of reactor coolant at a rate such that: (1) fuel and clad damage that could interfere with continued effective core cooling is prevented and (2) clad metal-water reaction is limited to negligible amounts.

Section 50.46 of 10 CFR, "Acceptance Criteria for Emergency Core Cooling Systems for Light-water Nuclear Power Reactors," as it relates to the ECCS equipment being provided that refills the reactor vessel in a timely manner for a LOCA resulting from a spectrum of postulated piping breaks within the reactor coolant pressure boundary. The ECCS cooling performance following postulated LOCAs must be calculated in accordance with an acceptable evaluation model to demonstrate conformance to the following acceptance criteria set forth in 10 CFR 50.46(b):

- The calculated maximum fuel element cladding temperature does not exceed 1200 degrees Celsius (°C) (2200 degrees Fahrenheit (°F)).

- The calculated total local oxidation of the cladding does not exceed 17 percent of the total cladding thickness before oxidation. Total local oxidation includes pre-accident oxidation as well as oxidation that occurs during the course of the accident.

- The calculated total amount of hydrogen generated from the chemical reaction of the cladding with water or steam does not exceed one percent of the hypothetical amount that would be generated if all of the metal in the cladding cylinders surrounding the fuel, excluding the cladding surrounding the plenum volume, were to react.

- Calculated changes in core geometry are such that the core remains amenable to cooling.

- After any calculated successful initial operation of the ECCS, the calculated core temperature is maintained at an acceptably low value and decay heat is removed for the extended period of time required by the long-lived radioactivity remaining in the core.

Section 50.46(a)(1)(i) of 10 CFR, also requires that for the realistic analysis of the ECCS cooling performance, the uncertainties in the analysis method and input must be identified and assessed so that the uncertainty in the calculated results can be estimated and accounted for.

The APR1400 SIS design, including the SITs, must comply with GDC 35, and the cooling performance will be evaluated through the safety analyses of LOCA for the full spectrum of break sizes (including LBLOCA and small break LOCA) to demonstrate that the above acceptance criteria are met. The staff's approval of the APR1400 SIS design requirements, which are intended to comply with GDC 35, are not documented in this safety evaluation report (SER), but instead, will be documented in the SER of the applicant's LBLOCA topical report (Reference 6).

The staff's evaluation of this topical report (Reference 1) includes the evaluation of the uncertainties and applicability of the experimental results to APR1400 as part of the LOCA evaluation models for the calculation of the APR1400 ECCS capability, as required by 10 CFR 50.46 and GDC 35.

3.0 TECHNICAL EVALUATION

The APR1400 SIS configuration includes four SITs connected to the reactor coolant system (RCS) via the direct vessel injection (DVI) nozzles. In addition, four safety injection pumps (SIPs) inject directly into the reactor vessel downcomer following a safety injection (SI) actuation signal.

Each SIT-FD consists of a tank partially filled with borated water and pressurized with nitrogen, and a FD inside the tank at the tank exit. The FD consists of a vortex chamber, a partition plate for segregating large and small flow, a standpipe connected to the supply port, control ports which are open to the liquid in the SIT at all times, an exit nozzle connected to the outlet port of the vortex chamber and the injection pipe. The configuration and typical flow pattern of the SIT-FD design is shown in Figure 2.2-1, "Structure of the APR1400 SIT installed with the Fluidic Device," Figure 2.2-2, "Structure of the Fluidic Device," and Figure 2.2-3, "Illustration of a Typical Flow Pattern inside the Vortex Chamber (a) Large Flow Rate Condition (b) Small Flow Rate Condition," (Reference 1).

When a LOCA occurs and pressure in the reactor vessel decreases below the SIT pressure, the check valves in the injection pipe open to permit the injection of the SIT injection water into the reactor vessel. With the initial water level in the SIT higher than the elevation of the inlet to the standpipe, water flows into the vortex chamber through the large-flow rate supply nozzles and small-flow rate control nozzles. These flows collide with each other at a design facing angle between the large flow and small flow inlet nozzles of the vortex chamber to decrease angular momentum, thus preventing a strong vortex formation in the vortex chamber. Consequently, the flow resistance in the vortex chamber is small, resulting in a large flow rate.

The large-flow injection phase continues until the water level in the SIT falls below the inlet elevation of the standpipe, and the flow in the standpipe decreases rapidly. The flow from the small-flow control ports enters the vortex chamber tangentially through only the control nozzles, which creates a strong vortex in the vortex chamber. The vortex in the chamber creates a large resistance to flow, and therefore, results in a small-flow injection rate. The switching from the large-flow to small-flow injection phase is thus accomplished passively without any moving parts.

The APR1400 SIT is designed with two performance objectives: (1) immediately after the reactor coolant blowdown during a LBLOCA, the SIT injects borated water at a large flow rate for a limited duration of time to refill the reactor vessel lower plenum and downcomer, and (2) after the refill period, it injects water at a relatively small flow rate to establish the core reflooding condition by maintaining the downcomer water level. To achieve these performance objectives, Section 2.3, "Design Requirements of the SIT-FD," (Reference 1) describes the determination of the design parameters for the large flow and small flow injection phases, respectively, based on a hypothetical LBLOCA sensitivity analysis. The water volume above the top of the standpipe in the SIT is the large flow injection water volume needed to refill the reactor vessel lower plenum and downcomer during the refill phase of a LOCA. The injection flow rates for the large-flow and small-flow injection phases, respectively, are designed to refill the lower plenum and downcomer as rapidly as possible and to provide a sufficient reflood rate to assure the peak cladding temperature is within the acceptance criteria during the worst case LOCA as evaluated in Reference 6.

The design requirement for the total pressure loss coefficient of the SIT-FD injection flow path for the large flow phase is calculated based on the refill injection rate requirement, the SIT pressure, and the RCS depressurization transient. The design requirement for the total pressure loss coefficient of the SIT-FD injection flow path for the small flow phase is calculated based on the requirements of the minimum flow rate and injection duration to keep the downcomer filled with water and to preclude the core boil-off rate from exceeding the SIP injection rate. The FD pressure loss coefficients for the large-flow and small-flow phases, respectively, are obtained by subtracting the pressure loss coefficient of the SI line from the SIT-FD nozzle to the DVI nozzle from the total pressure loss coefficient of the FD and SI line combined. The LBLOCA sensitivity study establishes the design requirements for the target FD pressure loss coefficients and water injection volumes for the large-flow and small-flow injection phases, respectively. The design specifications of the SIT-FD as summarized in Table 3.1-1, "Specification of the SIT," of the topical report (Reference 1), includes additional margins from the results of the sensitivity analysis. Section 3.1, "Safety Injection Tank," presents the detailed design of the "as installed" SIT with the structure of the SIT-FD depicted in Figure 3.1-1, "Drawing of the SIT (Side View)," and Figure 3.1-2, "Drawing of the SIT (Top View)," of the topical report (Reference 1).

3.1 Evaluation of SIT Performance

3.1.1 Full Scale Tests

The FD is designed to act as a passive flow controller where flow decreases rapidly as the water level in the tank decreases below the height of the standpipe entrance. The applicant conducted four series of full-scale performance verification tests at the Valve Performance Evaluation Rig (VAPER) test facility at the Korea Atomic Energy Research Institute to confirm the operational principles of the FD, and examine the performance of the SIT-FD. The full scale test facility, VAPER, consists of the SIT installed with the FD, a compressed air supply system, SIT water discharge pipe line and associated valves, SIT water supply and recirculation system, stock tank, and a data acquisition and control system as shown in Figure 4.1-1, "Schematic of the VAPER Facility," of the topical report (Reference 1). The SIT of the VAPER facility was manufactured to have the same inner diameter, height, and volume of the APR1400 SIT. The

stock tank, which receives the discharged contents of the SIT during the tests, is kept at atmospheric pressure. No scaling analysis was needed.

Two series of tests, identified as the Case-01 series and the Case-02 series, correspond to the standard FD tests; that is, the FD in these two series of tests has almost the same geometrical dimensions as the FD of the APR1400, but the Case-02 series has a slightly higher stand pipe than the Case-01 series in order to examine the effect of the stand pipe height on FD performance. The other two series of tests, identified as the Case-03 series and the Case-04 series, are sensitivity tests to evaluate the effects of manufacturing tolerances. The details of the test objectives, test apparatus, and test results for these tests are described in Section 4, "Performance Verification Tests," of the topical report (Reference 1).

Three Case-01 tests were performed at the reference test conditions, shown in Table 4.2-1, "Reference Test Conditions for the Performance Verification Tests of the VAPER SIT," of the topical report, (Reference 1), in order to check the repeatability of the test results. One additional Case-01 test was performed at approximately half of the reference pressure in order to evaluate the reliability of the pressure drop characteristics of the FD. The test conditions of Case-01 tests are summarized in Table 4.2-2, "Test Conditions of Case-01 Tests," of the topical report (Reference 1). A total of four tests were performed as a part of the Case-01 series.

Three Case-02 tests were also performed at the reference test conditions to check the repeatability of the tests. Case-02 tests utilized a stand pipe which was approximately 12.87 inches higher than the stand pipe in Case-01. The test conditions for Case-02 are summarized in Table 4.2-3, "Test Conditions of Case-02 Tests," of the topical report (Reference 1). A total of three tests were performed as a part of the Case-02 series.

In addition, three Case-03 and three Case-04 sensitivity tests were performed at the reference test conditions to ensure repeatability of the tests. Case-03 tests utilized vortex chamber height reduction and Case-04 tests utilized vortex chamber height reduction as well as control nozzle width enlargement to assess the effect of maximum expected manufacturing tolerances. A total of three tests were performed as a part of the Case-03 series and a total of three tests were performed as a part of the Case-04 series.

Overall, these tests were performed with the objective of confirming the following characteristics:

- Principle and performance of SIT-FD.
- Passive injection flow control performance.
- Independence of pressure loss coefficient of the FD from initial pressure, height of stand pipe, and expected manufacturing tolerances.

A total of 13 tests were conducted as a part of the applicant's full-scale testing program for the SIT-FD system.

The staff reviewed the test facility setup, test cases, quality assurance program (QAP), and experimental procedures associated with the SIT-FD full scale testing program. The staff noted that the applicant designed the test cases to cover the major phenomena associated with the SIT-FD, such as, stand pipe height and initial internal pressure. The staff determined that the number and variety of test cases proposed by the applicant would be sufficient to validate whether or not the SIT-FD evaluated in the full-scale testing program could satisfy the design requirements of the APR1400. The staff noted that the QAP for the FD Performance Verification Tests were developed in accordance with 10 CFR Part 50 Appendix B and American National Standards Institute/American Society of Mechanical Engineers NQA-1-1994. The staff also noted that the experimental procedures associated with the SIT-FD full-scale testing program contained provisions for testing the repeatability of the experiments.

During a review of the applicant's full-scale test facility schematics, the staff discovered a discrepancy between the discharge pipe inside diameter of Figure A-5, "Drawing of the Discharge Pipe connected to the Exit Nozzle," and descriptions of the discharge pipe provided in Section 4.1.3, "Subsidiary Components," and Section 5.1, "Representative Pipe Area for the Fluidic Device K-Factor." Therefore, the staff issued Request for Additional Information (RAI) 2-7371, Question 13 (ADAMS Accession No. ML14100A668), to address this issue. In its response to RAI 2-7371, Question 13 (ML14104A001), the applicant stated that the figure was incorrect. In addition, the applicant provided the staff with the correct figure. In its revised response to RAI 2-7371, Question 13 (ML15166A379), the applicant showed the staff how the topical report (Reference 1) will be updated with the correct figure. Therefore, RAI 2-7371, Question 13, is being tracked as a confirmatory item pending the incorporation of the corrected figure into the topical report (Reference 1).

The staff accepts, pending the inclusion of the corrected figure into the topical report (Reference 1), that the applicant's full-scale test facility setup and testing procedures provide a sufficient and adequate means for testing the SIT-FD to validate whether or not it satisfies the APR1400 design requirements.

3.1.2 Performance of the FD during Large and Small Flow Phases

During a LOCA, there is initially large flow injection from the accumulator when the check valve in the injection pipe opens in response to the decrease in RCS pressure below the SIT pressure setpoint. The flow decreases, as the water level in the SIT decreases and the level reaches near the entrance to the standpipe. The large flow injection phase occurs as the combination of flow from the standpipe and the flow from the small-flow control ports. Due to the supply nozzle injection in conjunction with the control nozzle injection into the vortex chamber, no strong vortex is allowed to form and the net flow is radial in the vortex chamber, thus allowing for a small flow resistance. As the flow in the standpipe decreases, the majority of flow into the vortex chamber comes from the tangential control nozzles, thus forming a strong vortex with a large increase in flow resistance resulting in a lower injection flow rate. During the switching of flow from the large-flow to the small-flow injection phase, the water level in the standpipe undergoes a transient due to inertial effects. When the water level of the SIT drops below the top of the stand pipe, the water level in the stand pipe decreases abruptly and reaches the lowest level, from which it slightly recovers thereafter. Finally, the water level in the SIT decreases gradually due to the increase in flow resistance.

The staff reviewed the applicant's tests results to verify the performance of the FD during large and small flow injection phases. The staff noted that when the SIT water level was above the top of the standpipe, the injection flow rate was substantially larger than when the SIT water level was below the top of the standpipe. The staff also noted that the small flow injection phase lasted substantially longer than the large flow injection phase. Based on the review of the test results, the staff determined that the measured FD K-factors confirmed the injection flow rates, observed in both the large flow and small flow injection phases.

Based on the test results, the staff was unable to gather an understanding for cavitation at the throat of the exit nozzle of the FD. Therefore, the staff issued RAI 2-7371, Question 15 (ML14100A668), requesting that the applicant consider the effects of cavitation on the FD performance, since the performance of the SIT-FD can be affected by vaporous pocket formations impeding flow. In its partial response to RAI 2-7371, Question 15 (ML14104A001), the applicant committed to providing a subsequent technical report of a computational fluid dynamics (CFD) analysis with an evaluation of the effects of cavitation on FD performance. In its full response to RAI 2-7371, Question 15 (ML14164A169), the applicant submitted APR1400-K-A-NR-14005-P, Revision 0, "CFD Analysis of Fluidic Device," (Reference 2) which fulfilled this commitment. The CFD analysis qualitatively confirmed vaporous cavitation occurrence in the center of the exit nozzle in both large and small flow modes. The applicant's response included justification that the full-scale VAPER test results inherently include any effects due to cavitation. The staff evaluated the CFD analysis and confirmed the qualitative confirmations of vaporous cavitation occurrence. The staff accepts the conclusion that the full-scale experimental tests capture the effects of cavitation. Therefore, RAI 2-7371, Question 15, is resolved and closed.

Test Case-03 and Test Case-04 were conducted to analyze the effects of manufacturing tolerances on the FD K-factor. The staff noted that the experimental results show that the manufacturing tolerances, associated with Case-03 and Case-04, have an insignificant effect on the measured FD K-factor. The staff issued RAI 2-7371, Question 17 (ML14100A668), asking

the applicant about how the facing angle uncertainty of the nozzle design in the FD might affect the FD K-factor. The CFD analysis (Reference 2) also analyzed the effect of this manufacturing tolerance by varying the nominal facing angle. In its response to RAI 2-7371, Question 17 (ML14164A169), the applicant showed that the APR1400 design requirement range for the SIT-FD K-Factor bounds the CFD results. The staff evaluated the CFD analysis on the effect of the manufacturing tolerance of the facing angle and confirmed that the design requirements for the APR1400 SIT-FD, bound the computational results. Furthermore, the staff concluded that since the manufacturing tolerance uncertainties, as evaluated in the full scale tests, have an insignificant effect on the measured K-Factor, then the manufacturing tolerance of the facing angle will exhibit the same behavior; and ultimately, the design requirements for the SIT-FD will remain bounding. In addition, the random uncertainty included in the uncertainty analysis as part of the final K-Factor values accounts for manufacturing tolerances. Therefore, RAI 2-7371, Question 17, is resolved and closed.

The staff evaluated the full scale testing results and confirmed that the performance of the SIT-FD during large and small flow injection phases behaves as intended by the applicant's design. The results of these tests showed that a large flow rate manifests when the tank water level is above the standpipe; and when the water level in the tank falls below the inlet of the standpipe, the injection flow rate decreases significantly. The accompanying CFD analysis qualitatively confirms vortex formation inside the FD as well as cavitation effects during large and small flow injection phases. The staff's evaluation concludes that the design requirements of the APR1400 SIT-FD bound all full-scale experimental and computational results of the applicant's test program, and that cavitation is inherently accounted for in the full-scale testing. The staff's evaluation also confirmed the design principle of passive flow control by the FD.

3.1.3 Effect of Dissolved Nitrogen

Fluid in the SIT of the APR1400 is in contact with nitrogen and over time nitrogen will dissolve and diffuse throughout the liquid phase. In the limiting case, water becomes saturated with nitrogen at equilibrium. A potential impact of dissolved gas on the performance of the FD thus exists. As the fluid particles move through the FD, subject to a pressure drop, the dissolved nitrogen gas will emerge out of solution and potentially affect the flow resistance of the FD.

The applicant utilized compressed air as the cover gas and liquid water as the injection fluid. The staff noted that there was no attempt to test dissolved gas in equilibrium with the injection liquid. However, to evaluate the effect of dissolved nitrogen gas on the FD K-factor, the applicant provided an estimate of the dissolved nitrogen flow rate out of solution during the whole injection period. First, the applicant calculated the solubility of nitrogen in the SIT water for SIT water temperatures of 0 °C (32 °F) and 40 °C (104 °F) using the empirical correlation from "Prediction of Nitrogen Solubility in Pure Water and Aqueous NaCl Solutions up to High Temperature, Pressure, and Ionic Strength," (Reference 5). The staff noted that boron solubility was ignored in the applicant's analysis. The applicant assumed that the nitrogen gas content in the SIT water reaches the equilibrium state of the solubility given by the empirical correlation during the fast pressure transient process across the FD. Using data obtained from Case-01-01 data, the mass release rate of nitrogen from solution was computed over time for two different temperatures of 0 °C (32 °F) and 40 °C (104 °F). Due to the higher nitrogen gas solubility in water during the large flow rate period, the mass release rate of nitrogen gas was larger during

this time compared to the small flow rate period. In the applicant's experiments, it was observed that the air discharged through the empty stand pipe had little effect on the pressure loss coefficient. The applicant concluded that since the air discharge rate peaked at a higher rate than what was obtained from the dissolved nitrogen gas release rate calculation and that the air discharge had little effect on the pressure loss coefficient, then dissolved nitrogen released during the SI period would also have an insignificant effect on the observed pressure loss. The staff reviewed the applicant's dissolved nitrogen calculation and confirmed the applicant's conclusion based on the calculation results.

The staff identified a discrepancy in Table 5.2-1, "N_2 Solubility (kg/kg_{water}) in Pure Water at 0 C," and in Table 5.2-2, "N_2 Solubility (kg/kg_{water}) in Pure Water at 40 °C" (Reference 1). Both tables contained errors in the calculated nitrogen solubility. Therefore, on March 30, 2015, the staff had a clarification phone call with the applicant regarding the errors discovered in the tables. Subsequently, the applicant submitted a revised response to RAI 2-7371, Question 16 (ML15113A290), which corrected the errors in Tables 5.2-1 and 5.2-2. Therefore, RAI 2-7371, Question 16, is being tracked as a confirmatory item pending the incorporation of the corrected nitrogen solubility calculations into Table 5.2-1 and Table 5.2-2 (Reference 1).

Based on the review of the applicant's dissolved nitrogen effect calculation, the staff determined that the calculation's results are acceptable, pending the inclusion of the corrected nitrogen solubility calculations, and approves the applicant's conclusion regarding the insignificance that dissolved nitrogen has on the pressure loss coefficient.

3.1.4 Uncertainty Analysis

The total uncertainty of the pressure loss coefficient developed from the full-scale testing of the FD was computed by systematically evaluating uncertainty contributions from many parameters including, but not limited to, water injection flow rate and pipe cross sectional area. The uncertainties were analyzed at a 95 percent confidence level.

The systematic uncertainty of the SIT water injection flow rate was evaluated by a propagation of the elemental uncertainty sources (water density, SIT cross-sectional area, and SIT water level). The systematic uncertainty of the pressure loss coefficient of the FD was also evaluated through a propagation of the elemental uncertainty sources (FD pressure drop, water density, pipe cross sectional area, and water injection flow rate). The random uncertainty of the pressure loss coefficient of the FD was evaluated by multiplying the coverage factor of the student *t*-distribution with a degree of freedom of 12 (13 total test cases minus 1) with the standard deviation of the pressure loss coefficients from all the test cases. The random uncertainty accounts for the effects of process unsteadiness, differences in test conditions, and manufacturing tolerances. Finally, the total uncertainty of the pressure loss coefficient of the FD was estimated by the root sum square of the systematic and random uncertainties. The applicant's uncertainty analysis concluded that the experimental test results plus uncertainty fall within the design requirement ranges for the APR1400. The staff reviewed and accepts the applicant's uncertainty analysis and confirms that the APR1400 design requirements bound the test results plus uncertainty.

4.0 CONCLUSION

The staff reviewed APR1400 Topical Report APR1400-Z-M-TR-12003-P, Revision 0, "Fluidic Device Design for the APR1400," (Reference 1), as well as the responses to the staff's RAIs. As a result of its review, the staff reached the following conclusions:

a) The full-scale test facility provides a sufficient and adequate means for testing the SIT- FD to validate whether or not it satisfies the APR1400 design requirements.

b) The full scale tests demonstrate and confirm that the SITs injection flow is passively controlled by a FD.

c) The performance and design of the SIT-FD evaluated in the full-scale VAPER test facility satisfies the design requirements of the APR1400 SIT-FD, which are intended by the applicant to meet the criteria provided in GDC 35 and 10 CFR 50.46.

d) The applicant has shown that manufacturing tolerances and dissolved nitrogen provide an insignificant effect on the observed pressure loss coefficient of the FD.

e) The applicant has shown that the design requirements of the APR1400 bound all full-scale experimental and computational results with uncertainties.

RAI 2-7371, Questions 13 and 16, are being tracked as confirmatory items pending the incorporation of a corrected figure and a corrected table in the topical reports (Reference 1). Overall, the staff considers the design, testing, and evaluation of the SIT-FD acceptable with limitations identified below.

5.0 LIMITATIONS

The staff's approval of the APR1400 SIS design requirements, which are intended by the applicant to comply with GDC 35 and 10 CFR 50.46(b), is not documented in this SER, but instead, is pending the approval of the applicant's LBLOCA topical report (Reference 6). The safety evaluation conducted by the staff and presented herein approves the applicant's development of the SIT-FD in conformance with a specific set of design and performance requirements of the APR1400.

6.0 REFERENCES

1. "Fluidic Device Design for the APR1400," APR1400-Z-M-TR-12003-P, Revision 0, issued December 2012 (ML13018A194).

2. "CFD Analysis of Fluidic Device," APR1400-K-A-NR-14005-P, Revision 0, issued June 2014 (ML14164A170).

3. ANSYS CFX 14.5 Documentation, "Theory Guide," issued November, 2011.

4. ANSYS CFX-Solver Theory Guide, Release 12.1, issued November, 2009.

5. R. Sun, W. Hu, Z. Duan, "Prediction of Nitrogen Solubility in Pure Water and Aqueous NaCl Solutions up to High Temperature, Pressure, and Ionic Strength," Journal of Solution Chemistry, Vol. 30, No. 6, pp. 561-573, issued 2001.

6. "Realistic Evaluation Methodology for Large-Break LOCA of the APR1400," APR1400-F-A-TR-12004-P, Revision 0, issued December 2012 (ML13023A081).

7.0 LIST OF ACRONYMS

ADAMS	Agencywide Documents Access and Management System
APR1400	Advanced Power Reactor 1400
CFD	Computational Fluid Dynamics
CFR	Code *of Federal Regulations*
DVI	Direct Vessel Injection
ECC	Emergency Core Cooling
ECCS	Emergency Core Cooling System
FD	Fluidic Device
GDC	General Design Criteria
LBLOCA	Large Break Loss-of-Coolant Accident
LOCA	Loss-of-Coolant Accident
NRC	U. S. Nuclear Regulatory Commission
PWR	Pressurized Water Reactor
QAP	Quality Assurance Program
RAI	Request for Additional Information
RCS	Reactor Coolant System
SER	Safety Evaluation Report
SI	Safety Injection
SIP	Safety Injection Pump
SIS	Safety Injection System
SIT	Safety Injection Tank
SIT-FD	Safety Injection Tank with Fluidic-Device
VAPER	Valve Performance Evaluation Rig

Page intentionally left blank

SECTION B

Page intentionally left blank

Fluidic Device Design for the APR1400 (Approved Version)

Non-Proprietary

April 2017

ABSTRACT

This topical report provides the design specifications and working principles of the flow controlling fluidic device (FD) which has been adopted in Advanced Power Reactor 1400 (APR1400) design. The FD is installed inside the pressurized safety injection tank (SIT) of APR1400, and it passively controls the water injection flow rate from the SIT. The FD primarily consists of a stand pipe and a vortex chamber. The vortex chamber can receive injection water through control ports as well as through the stand pipe. When the SIT water level is above the top of the stand pipe, water enters the vortex chamber through both the top of the stand pipe and the control ports resulting in injection of water at a large flow rate. When the water level drops below the top of the stand pipe, water only enters the vortex chamber through the control ports resulting in vortex formation in the vortex chamber and a relatively small flow injection. Therefore, the SIT provides short term large flow injection to refill the reactor vessel and then a smaller flow injection which, in conjunction with the safety injection pump (SIP), adequately supports the core reflooding phase. The FD improves the loss of coolant accident (LOCA) safety analysis by reducing the amount of SIT safety injection (SI) water that would spill into the containment once the downcomer is full, thereby, improving the overall reliability of SI water injection.

The performance of the FD has been also evaluated by repeated experiments in the full-scale Valve Performance Evaluation Rig (VAPER) test facility at the Korea Atomic Energy Research Institute (KAERI). The experimental results confirm that the currently developed FD satisfies the major performance requirements of the APR1400 plant design regarding the injection flow rate, pressure loss coefficient (K-factor), and injection duration time. Basically, the pressure loss coefficient of the small flow rate period is almost [ ]^{TS} higher than that of the large flow rate period due to the strong vortex motion in the FD. The K-factor of the safety injection system (SIS) in APR1400 has been evaluated based on the K-factor obtained from the tests, and this value essentially matches the target design value of the SIS in the APR1400.

A quality assurance program for the FD tests has been applied to assure the high quality of the experimental results.

TABLE OF CONTENTS

LIST OF TABLES

LIST OF FIGURES

ULIST OF ACRONYMS

ANS	American Nuclear Society
ANSI	American National Standards Institute
APR1400	Advanced Power Rector 1400
ASME	American Society of Mechanical Engineering
CEA	Control Element Assembly
CFR	Code of Federal Regulations
DVI	Direct Vessel Injection
ECC	Emergency Core Cooling
FD	Fluidic Device
IRWST	In-containment Refueling Water Storage Tank
KAERI	Korea Atomic Energy Research Institute
KEPCO E&C	Korea Electric Power Corporation Engineering & Construction Company
KEPCO NF	Korea Electric Power Corporation Nuclear Fuel Company
KHNP	Korea Hydro & Nuclear Power Corporation
LBLOCA	Large Break LOCA
LOCA	Loss of Coolant Accident
LPSIP	Low Pressure Safety Injection Pump
M&TE	Measuring & Test Equipment
PCT	Peak Cladding Temperature
POSRV	Pilot Operated Safety and Relief Valve
RCS	Reactor Coolant System
SBLOCA	Small Break LOCA
SDVS	Safety Depressurization and Vent System
SI	Safety Injection
SIAS	Safety Injection Actuation Signal
SIP	Safety Injection Pump
SIS	Safety Injection System
SIT	Safety Injection Tank
SIT-FD	Safety Injection Tank with the Fluidic Device
USNRC	United States Nuclear Regulatory Commission
VAPER	Valve Performance Evaluation Rig

1. INTRODUCTION

This report describes the fluidic device (FD) design used in Advanced Power Reactor 1400 (APR1400). KHNP intends to seek certification of the APR1400 design from the United States Nuclear Regulatory Commission (USNRC). The purpose of this topical report is to provide the design details and confirmatory testing results of the FD to the USNRC in order to facilitate the review of this innovative design in advance of the submission of the APR1400 Design Certification Application.

The safety injection tank with the fluidic device (SIT-FD) is an accumulation tank which is partially filled with borated water and is pressurized with nitrogen, with the FD located at the tank exit. It is connected to the reactor coolant system (RCS) with a series of check valves and an isolation valve and is aligned during plant normal operation to allow flow into the RCS if the RCS pressure drops below the pressure of the safety injection tank (SIT). The SIT-FD design combines known FD technologies and extensive operating experience of conventional accumulators used for loss of coolant accident (LOCA) mitigation in pressured water reactors. The passive FD located inside the SIT provides the inherent reliability to achieve a desired reactor coolant injection profile without the need for any active components. The injection profile is also optimized to limit the period of high flow injection to the time required to refill the downcomer. The remaining SIT water is then injected over a longer period to adequately remove decay heat from the core until the SIPs can take over this function

Incorporation of the SIT-FD into the APR1400 design and LOCA mitigation strategy simplifies an important safety system by integrating an inherently reliable passive safety component with the conventional safety injection system (SIS). This design improvement in addition to the direct vessel injection (DVI) contributes to the elimination of Low Pressure Safety Injection Pumps (LPSIPs) in APR1400. It is also expected that the use of SIT-FD in the APR1400 design will reduce the net maintenance and testing workload at nuclear facilities while maintaining a very high level of safety.

This report includes the basic operation principles of the FD, the important design features, and the confirmative testing program results which assure the performance of the SIT-FD.

2. DEVELOPMENT PROGRAM OF THE FLUIDIC DEVICE

2.1 Background of the Fluidic Device Development

Evolutionary nuclear power reactors have been developed since the 1980's. One of the main characteristics of these new reactor types is the improvement and expansion of passive components. The passive components decrease the complexity of the SIS and improve the reliability of the system.

Conventional nuclear power plants were designed to deliver cooling water into a reactor vessel from SITs in the refill phase, and to deliver the cooling water by safety injection pumps (SIPs) during the reflood phase in the event of a Large Break Loss of Cooling Accident (LBLOCA) (Figure 2.1-1). During a LBLOCA, the fuel cladding temperature increases since the liquid around the core is carried away by a significant loss of reactor coolant from the RCS. The SIS is required to inject cooling water into the core to limit the fuel temperature increase. SI water in the SIT plays the role of rapidly raising of the water level in the downcomer up to the cold leg bottom in the refill stage, removing decay heat of the reactor core and sensible heat of the nuclear fuels and metal structures in the early reflood phase. The SITs of conventional nuclear power plants deliver excessive cooling water to the reactor vessel after the water level has been raised to the cold leg bottom elevation, causing SI water to flow into the containment atmosphere. This excess flow to the containment limits the usefulness of SI water and can cause a decrease in the reflood rate.

Shin-Kori Unit 3, the first nuclear power plant based on APR1400 is scheduled to be in commercial operation in the year of 2013 in Korea. APR1400, with the power capacity of 1400 MWe, has adopted new design features. One of the new design features is four mechanically independent trains for the SIS. In addition, each of the four SITs of APR1400 has a FD which passively controls the injection flow rate into the reactor coolant system during refill and reflood phases (i.e., a large injection flow rate during the refill phase and a small injection flow rate during the reflood phase). The flow control mechanism of the FD is due to a change in the flow resistance inside a vortex chamber of the FD. Figure 2.1-1 shows the SI flow rate with time during a LOCA relative to the minimum requirement to support rapid refill, reflood and sustained core cooling.

The system configuration of the SIS of APR1400 is shown in Figure 2.1-2. The SIS consists of four mechanically separated trains, and associated valves, piping and instrumentation. Each train contains one SI pump, one SIT, and associated suction and discharge paths.

Each SI pump is provided with its own suction line from the In-containment Refueling Water Storage Tank (IRWST) independently, and its own discharge line to a DVI nozzle on the reactor vessel. The SI pumps are sized such that for breaks, up to a double-ended guillotine break, two SI pumps in conjunction with the SITs through two diagonally located DVI nozzles provide the required minimum injection flow rate to the core to meet the system functions.

The passive portion of the SIS consists of four identical pressurized SITs. Four SITs initially provide a means of rapid reflooding of the core following a large break LOCA, and keeping it covered until the flow from the SI pumps becomes available. Each SIT contains borated water to a maximum of 2.5 weight percent boric acid and is pressurized with nitrogen to a nominal pressure of 4.21 MPa(g) (610 psig). The SITs are provided with connections for filling, draining, pressurizing, venting, relieving, and sampling. In addition, pressure and level instrumentations with appropriate alarms are provided to assure that Technical Specifications are met during normal power operation.

The SIS is also capable of injecting borated water into the reactor vessel to mitigate accidents other than LOCAs. Safety injection would be initiated in the event of a Steam Generator Tube Rupture, Steam Line Break or a Control Element Assembly (CEA) Ejection incident. The borated water injected by the SIS provides inventory and reactivity control for these events.

A prototypical full-scale test facility at the Korea Atomic Energy Research Institute (KAERI), called Valve Performance Evaluation Rig (VAPER), was used to evaluate the flow controlling performance of the APR1400 FD. KAERI has performed various thermal hydraulic tests to evaluate and verify the performance of this new APR1400 design feature. The test results will be shown in Chapter 4.

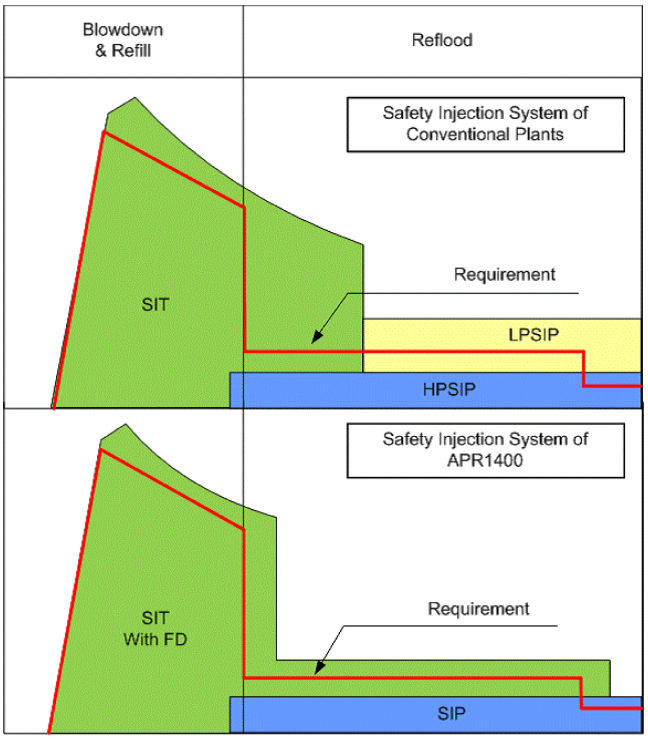

Figure 2.1-1 SI Flow Rate with Time during a LOCA

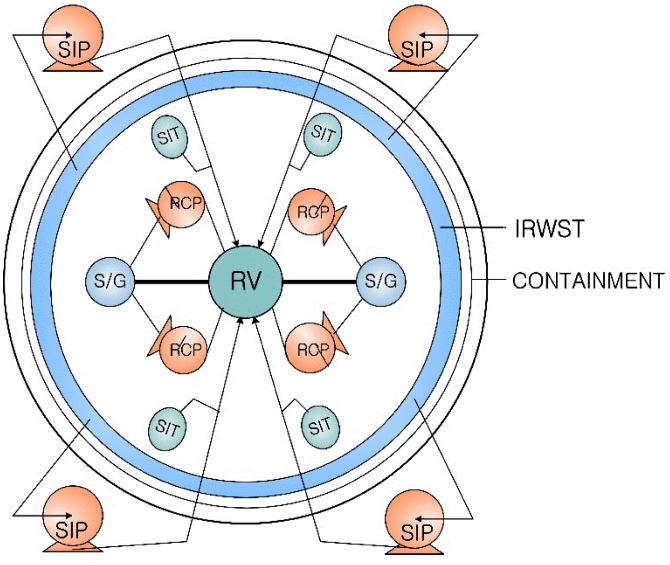

Figure 2.1-2 System Configuration of the SIS of the APR1400

2.2 Working Principles of the Fluidic Device

The structures of the APR1400 SIT and the FD are presented in Figures 2.2-1 and 2.2-2, respectively. Flow patterns inside the vortex chamber are illustrated in Figure 2.2-3. The FD is installed at the bottom part of the SIT. The FD has a supply port at the center and four control ports around the supply port with an equal circumferential angle of 90^{o} at the surface top. The supply port is connected to a stand pipe that extends vertically.

The SIT water delivered through the supply port is divided into four directions with a relative angle of [ ]^{TS} by a partition plate (Figure 2.2-2), and then flows into the vortex chamber through four supply nozzles (Figure 2.2-3). On the other hand, the SIT water delivered through the four control ports flows directly into the vortex chamber through four control nozzles (Figures 2.2-1 ~ 2.2-3). Finally, the SIT water is discharged through an exit nozzle at the bottom center of the vortex chamber.

Control nozzles inject SIT water tangentially into the vortex chamber, establishing a strong swirling flow inside the vortex chamber when SIT water is only injected through the control nozzles (Figure 2.2-3 (b)). This causes a high flow resistance through the FD. In contrast to the control nozzle, each supply nozzle has an angle of [ ]^{TS} with a neighboring control nozzle in order to minimize the swirling flow effect (Figure 2.2-3 (a)). Consequently, the flow resistance through the FD is significantly decreased when SIT water is delivered into the vortex chamber through both the supply and control nozzles.

SIT water is delivered into the vortex chamber through both the supply and control nozzles at the early stage of LBLOCA when the SIT starts to operate and the stand pipe is covered with water. The SIT provides a large injection flow rate of SIT water which is required during the refill phase of LBLOCA. When the SIT water level is lowered to below the top of the stand pipe, the flow path via the supply nozzle is absent and all SIT water is delivered only through the control nozzle. As a result, the injection flow rate of the SIT water is decreased, but is still sufficient to remove decay heat during the reflood phase, extending the total duration of the SIT water injection.

The APR1400 SIT-FD passively controls the injection flow rate of the SIT water without any moving part or any action of the plant operator with the help of the FD.

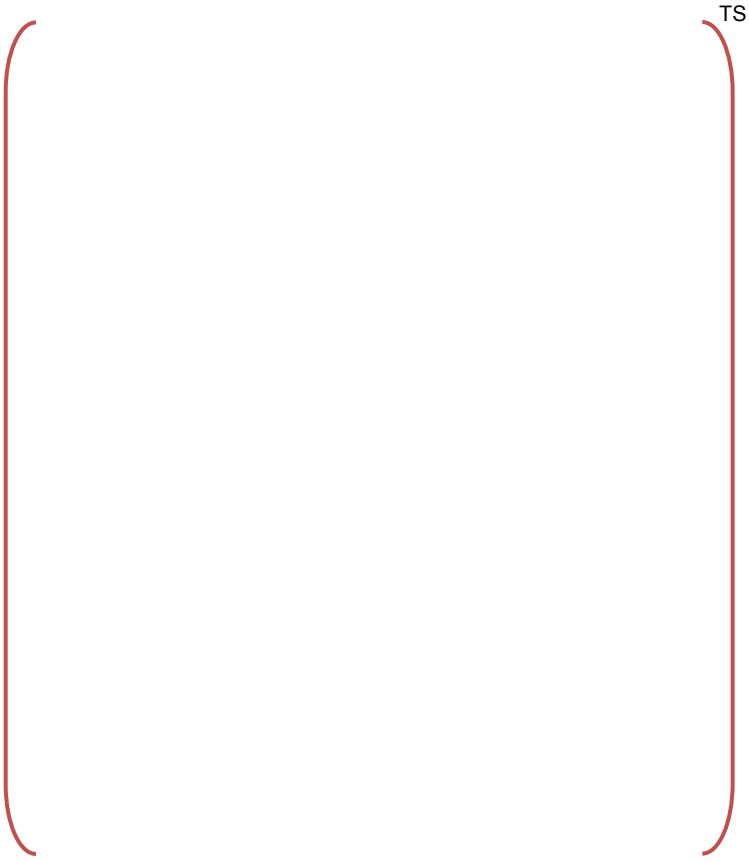

Figure 2.2-1 Structure of the APR1400 SIT installed with the Fluidic Device

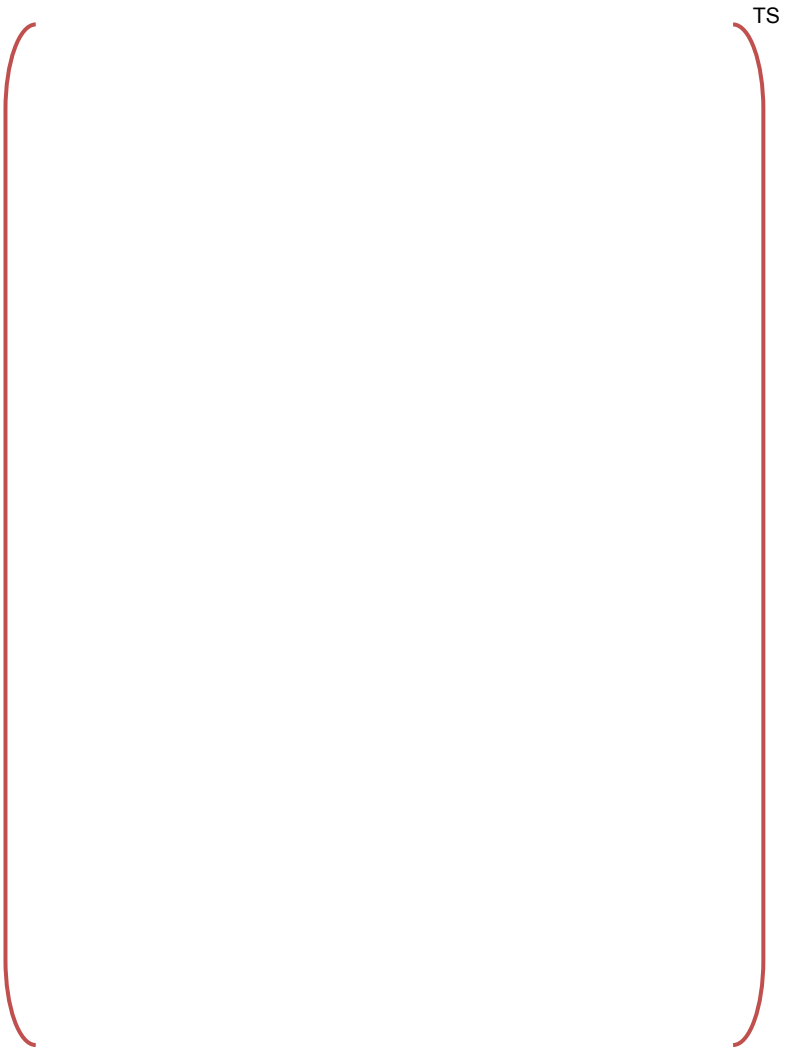

Figure 2.2-2 Structure of the Fluidic Device

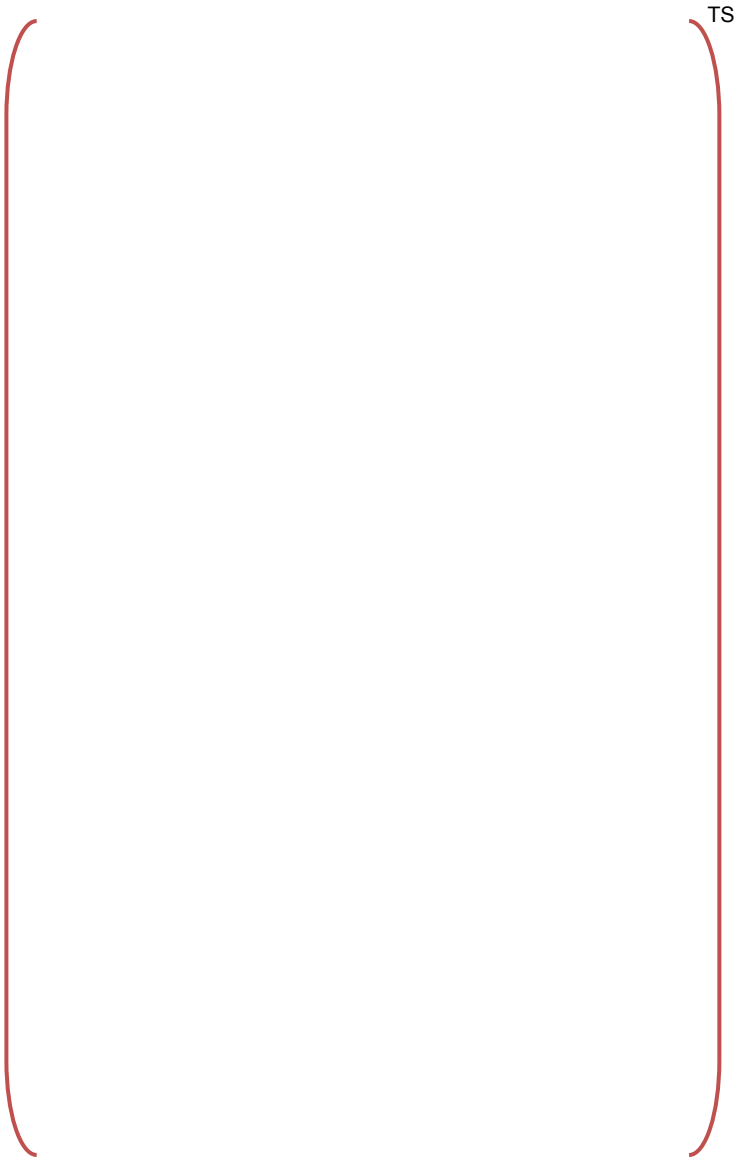

Figure 2.2-3 Illustration of a Typical Flow Pattern inside the Vortex Chamber
(a) Large Flow Rate Condition (b) Small Flow Rate Condition

2.3 Design Requirements of the SIT-FD

The SIT-FD should inject a large flow, for a limited duration in order to refill the reactor vessel lower plenum and downcomer, as rapidly as possible following the blowdown period and inject a relatively small flow to establish the core reflooding condition by maintaining the downcomer water level after refilling the reactor vessel lower plenum and downcomer.

In this section, the design requirements of SIT-FD are quantified by performing the hypothetical LBLOCA analysis and conservative assumptions. The limiting break, 100% double ended guillotine break in a cold leg, was considered in the analysis. The limiting break size was determined from the break size sensitivity study; this study considered 100 %, 80 % and 60 % double ended guillotine break in a cold leg, 100 % double ended guillotine break in a hot leg, 100 % double ended guillotine break in a pump suction leg, and 200% slot break in a cold leg (i.e., break is two times of the cold leg cross sectional area). The analysis was performed using the RELAP5/MOD3.3 code.

The total volume, the range of initial gas pressure and the range of available water volume of SIT-FD were determined by evaluating the volume of SIT water required to meet the stated acceptance criteria for the spectrum of LOCA break sizes performed for the APR1400.

- SIT-FD total volume: [ ]TS
- Range of initial gas pressure: [ ]TS
- Range of available water volume: [ ]TS

2.3.1 Design Requirements for Large Flow Injection

Core reflood begins after refilling the reactor vessel lower plenum and some portions of the downcomer (i.e., after a refill period). Since the reactor core is subject to adiabatic heat-up during the refill period, the duration of the refill period is one of the dominant factors determining reflood peak cladding temperature (PCT). The longer refill period will result in the higher reflood PCT. To shorten the refill period (core adiabatic heat-up period) and to reflood the core as rapidly as possible, the reactor vessel lower plenum and the downcomer should be filled by large flow rate injection from the SIT-FD. Therefore, the performance requirement for the large flow injection of SIT-FD is determined as follows:

- Injection with large flow rate should continue until the end of the refill period in order to fill the lower plenum and the downcomer as rapidly as possible.

Because the following parameters govern the duration of large flow injection, it is necessary to determine the design requirements of these parameters in order to meet the performance requirement, except the gas pressure that the effectiveness is confirmed by the sensitivity study.

1) Water volume above the top of the stand pipe
2) Initial gas pressure
3) Pressure loss coefficient of the flow path

In order to determine the design requirements for the governing parameters of large flow injection and to confirm their effectiveness, various LBLOCA analyses were performed for the limiting break size of 100 % double ended guillotine break in a cold leg. All combinations of the predetermined minimum and maximum values of water volume and gas pressure were used as initial SIT-FD conditions in the analyses.

- Water volume above the top of the stand pipe

During the LBLOCA of APR1400, the reactor coolant system (RCS) pressure decreases to near the containment pressure within about 40 seconds after break initiation and the pressure difference between the RCS and the containment becomes less than 0.05 MPa (7.3 psi) at 40 seconds. To

overcome this pressure difference of 0.05 MPa (7.3 psi) and to begin reflooding, the water head in the downcomer should be greater than 0.05 MPa (7.3 psi, equivalent to about 5 m (16.4 ft) of water column). Therefore, the minimum water volume above the top of the stand pipe was determined as; the water volume required to fill the lower plenum plus 5 m (16.4 ft) of the downcomer plus any losses due to emergency core cooling (ECC) bypass, etc. The minimum water volume required for large flow injection was obtained from the LBLOCA analysis in order to consider various thermal-hydraulic phenomena including the ECC water bypass in the downcomer. The calculated water volume to fill two regions was [ ]TS. To provide some additional margin, the final minimum water volume for large flow injection was determined as total[ ]TS or [ ]TS per each SIT-FD. This minimum water volume is large enough compared to the total volume 44.03 m^3 (1,555 ft^3) of the lower plenum and the lower downcomer below the cold leg elevation, to account for uncertainties, spillage, bypass, etc..

- Pressure loss coefficient of the flow path

The range of available water volume for large flow injection can be obtained using the previously determined minimum water volume above the top of the stand pipe and the available SIT water volume with the range of [ ]TS. The maximum water volume for large flow injection is calculated by subtracting the water volume below the top of the stand pipe from the maximum available water volume. Water volume below the top of the stand pipe of [ ]TS is obtained by subtracting the minimum water volume for large flow injection [ ]TS from the minimum available water volume [ ]TS. Therefore, the range of available water volume for large flow injection is obtained as [ ]TS. To effectively inject this available water while satisfying the performance requirement, an appropriate injection flow rate should be determined. The results of the APR1400 LBLOCA sensitivity study showed that the injection flow rate does not significantly affect the reflood beginning time because the system pressure decreases to near the containment pressure within 40 seconds after break initiation. In case of injection with a too low flow rate, however, the downcomer water level at the reflood beginning time was low and this resulted in a low initial core reflood rate. On the other hand, in case of injection with a too high flow rate, the large flow injection ended before the reflood beginning time. Therefore, the range for the peak flow for large flow injection was determined as [ ]TS based on the results of the sensitivity study. The range of the peak flow was satisfied if the total pressure loss coefficient of the FD and SI line from the SIT-FD nozzle to the DVI nozzle is between [ ]TS, for all the predetermined SIT-FD conditions. Since the range of the pressure loss coefficient of the expected SI line from the SIT-FD nozzle to the DVI nozzle is 6 ~ 10 Note1, the required range of the pressure loss coefficient of the FD during large flow injection is determined as [ ]TS and this range of the FD is specified as a design requirement.

Design Requirements for Large Flow Injection

- [ ]TS
- [ ]TS

[ ]TS

2.3.2 Design Requirements for Small Flow Injection

The dominant factor which determines the core reflood rate is the downcomer water level. Since the downcomer water level (i.e., water head) forces SI water into the core through the reactor vessel lower plenum, it is important to keep the downcomer filled with SI water in order to ensure a water

head for core cooling. The small flow injection should be continued until the SI flow rate from SIPs is higher than the core boil-off rate caused by decay heat, in order to keep the core adequately cooled.

Thus the performance requirements for small flow injection of the SIT-FD are determined as follows:

- The injection flow rate should be large enough to keep the downcomer filled with water.
- The injection should be continued until the SI flow rate from SIPs is higher than the core boil-off rate caused by decay heat.

These performance requirements can be satisfied by guaranteeing the minimum small flow rate and the minimum duration of small flow injection.

The required minimum small flow rate and the minimum duration of small flow injection were conservatively determined with enough margins, as follows:

- Minimum duration of small flow injection

Figure 2.3-1 shows the nominal SI flow rate from one SIP and the core boil-off rate by decay heat. The required minimum duration of small flow injection was defined so that small flow injection should be continued until the SI flow rate from one SIP exceeds the boil-off rate considering sufficient margin and ECC bypass. 1.2 times the ANS-79 decay heat model and the latent heat at atmospheric pressure were conservatively used in the calculation of the boil-off rate. Constant SI flow rate of 74 kg/sec (163.1 lb/sec), which is expected to be discharged at 0.45 MPa(a) (64.7 psia), was compared with the boil-off rate. The downcomer pressure decreases to 0.2 MPa(a) (29 psia) ~ 0.15 MPa(a) (21.8 psia) during the reflood. However, the downcomer pressure of 0.45 MPa(a) (64.7 psia) was assumed for a conservative SIP injection flow rate. After 112 seconds from the break initiation, the SI flow rate from one SIP exceeds the boil-off rate. Based on this, it was determined that the small flow injection should be continued until [ ]^{TS} after break initiation.

- Minimum injection flow rate

The required minimum small flow rate to maintain a full downcomer water level, once it has been refilled, can be determined based on the core boil-off rate by decay heat and the core reflood rate. The predetermined SIT conditions including the requirements for the large flow injection allow that the large flow injection continues at least until [ ]^{TS} after break initiation. The core boil-off rate conservatively calculated at [ ]^{TS} is less than 100 kg/sec. This implies that the small injection flow rate from four SIT-FDs should be higher than 100 kg/sec. Meanwhile, the minimum small flow rate can be calculated from the sum of the product of flow area times the reflooding rate of the core region and core shroud region. The reflooding rate of each region can be obtained from the LBLOCA analysis for the limiting break size of 100 % double ended guillotine break in a cold leg. The initial reflooding rate is faster because the power of the lower core region is relatively lower and the system pressure is kept at a low level before massive steam is generated in the core. Therefore, the initial reflooding rate, which was calculated when collapsed core water level reached [ ]^{TS} from the bottom of the core, was applied to the calculation of the minimum flow rate for the entire reflood period in order to consider enough margin. Based on the core boil-off rate and the calculation result, the minimum flow rate of [ ]^{TS} from each SIT-FD was determined. This minimum flow rate of [ ]^{TS} from one SIT-FD should be kept until [ ]^{TS} after break initiation. The safety injection from the SIPs will be the additional margin.

[ ]^{TS}

[ ] TS

Design Requirements for Small Flow Injection

- [ ] TS

[ ] TS

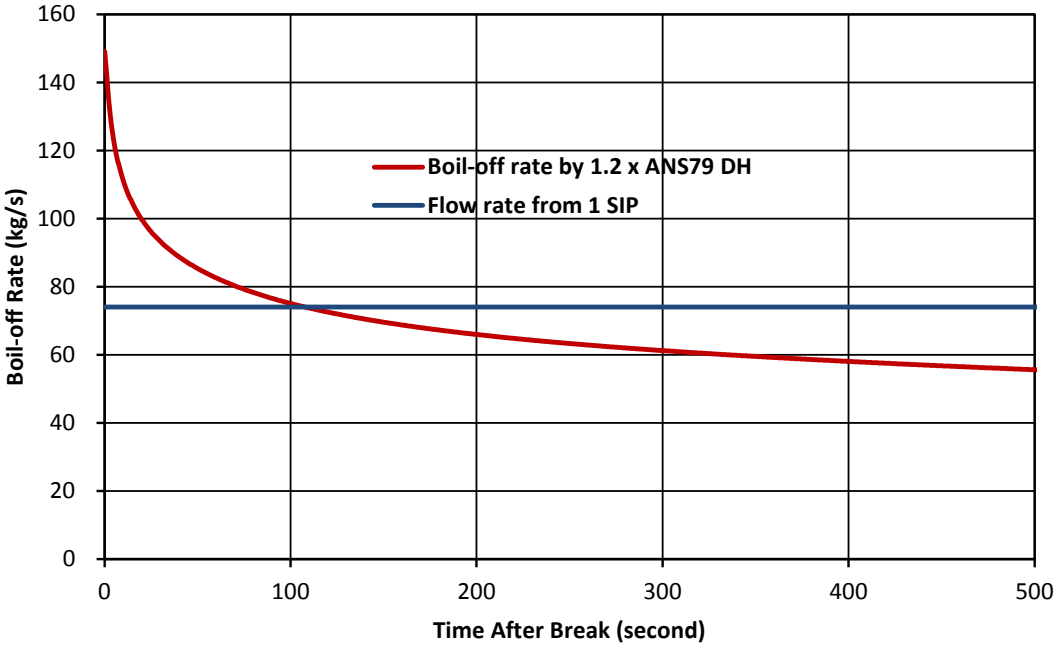

Figure 2.3-1 Boil-off Rate Resulting from 1.2 x ANS79 Decay Heat

3. DETAILED DESIGN OF THE SIT-FD

The design requirements of the APR1400 SIT-FD for large flow injection and small flow injection are described in Section 2.3. This Chapter describes the detailed design of the SIT-FD.

3.1 Safety Injection Tank

Each SIT connects to the reactor downcomer through one of the DVI nozzle, and has the function of injecting SIT water into the core at a large flow rate during the refill phase and at a small flow rate during the reflood phase.

The APR1400 SIT is designed to satisfy the design requirements specified in Section 2.3. The SIT has an inner diameter of [ ]^{TS} and a height of [ ]^{TS}. The SIT volume, design pressure and temperature are provided in Table 3.1-1. Detailed drawings of the SIT are shown in Figures 3.1-1 and 3.1-2.

The discharge piping of each SIT is routed to a DVI nozzle on the reactor vessel. The SITs automatically inject their contents of borated water into the RCS if the RCS pressure drops below SIT pressure as a result of a LOCA. Two check valves in the SIT discharge piping isolate the SITs from the RCS during normal plant operation. A motor-operated isolation valve provided in each SIT discharge line is administratively controlled open in the main control room to ensure SIT availability during normal operation. Power to each valve's motor operator is removed to prevent inadvertent closure. To further ensure SIT availability, each SIT isolation valve will receive an automatic open signal, should a safety injection actuation signal (SIAS) occur due to either low pressurizer pressure or high containment pressure. Each motor-operated SIT isolation valve is also provided with an "auto-open" and "permissive close" interlock based on pressurizer pressure. During startup, the interlock will automatically open the valves when the RCS pressure is increased above 4.14 MPa(a) (600 psia). During plant cooldown, the interlock will prevent the valves from being closed until the RCS pressure is reduced to 3.28 MPa(a) (475 psia).

The SITs are normally pressurized to a nominal operating pressure of 4.21 MPa(g) (610 psig) for normal operation. During startup, the operator will pressurize the SITs when pressurizer pressure reaches 4.41 MPa(a) (640 psia). Failure to do so will result in an alarm when pressurizer pressure reaches 4.93 MPa(a) (715 psia). During plant cooldown, SIT pressure is reduced to 2.76 MPa(g) (400 psig) when the RCS pressure reaches 4.41 MPa(a) (640 psia). Inadvertent repressurization of the SITs during this mode of operation, due to a leaky nitrogen supply valve or by accidental tripping of a nitrogen supply valve switch, is prevented by having two fail-closed valves in series with separate hand switches on each SIT nitrogen supply line. The air supply to actuate the nitrogen supply valves is controlled by solenoid valves. The two nitrogen supply valve solenoids on each SIT are connected to separate electrical buses via redundant and physically separated electrical trains. This is to ensure that a fault in one of the trains will not cause a spurious opening of both nitrogen supply valves. The SITs contain borated water at a maximum concentration of 2.5 weight percent boric acid (4,400 ppm).

The SIT gas/water fractions, gas pressure, and outlet pipe size are selected to flood and cover the core before significant fuel damage occurs and a significant zirconium-water reaction occurs following a LOCA. Redundant level and pressure instrumentation are provided to monitor the condition of the SITs. Sufficient visual and audible indications are made available to the operator such that maintaining the SITs within the required Technical Specifications during various modes of plant operation is readily accomplished from the main control room. Provisions have been made for sampling, filling, draining, and correcting boron concentration. Atmospheric vent valves are provided for SIT venting. They are locked closed and the power to each valve is removed during normal operation. This prevents inadvertent SIT venting during normal plant operation.

Table 3.1-1 Specification of the SIT

	TS
Type	
Number	
Code Class/Seismic Class	
Design Pressure	
Operating Pressure	
Design Temperature	
Operating Temperature	
Total Internal Volume	
Normal Fluid Volume[Note1]	
Maximum Fluid Volume[Note1]	
Minimum Allowable Fluid Volume[Note1]	
Minimum Fluid Volume above the Top of the Stand Pipe	
Minimum Allowable Dead Volume	
Discharge Piping K-factor	

Note 1: The volume of the FD itself including the stand pipe with support is not included. The volume below the FD control port (dead volume) is not included, either.

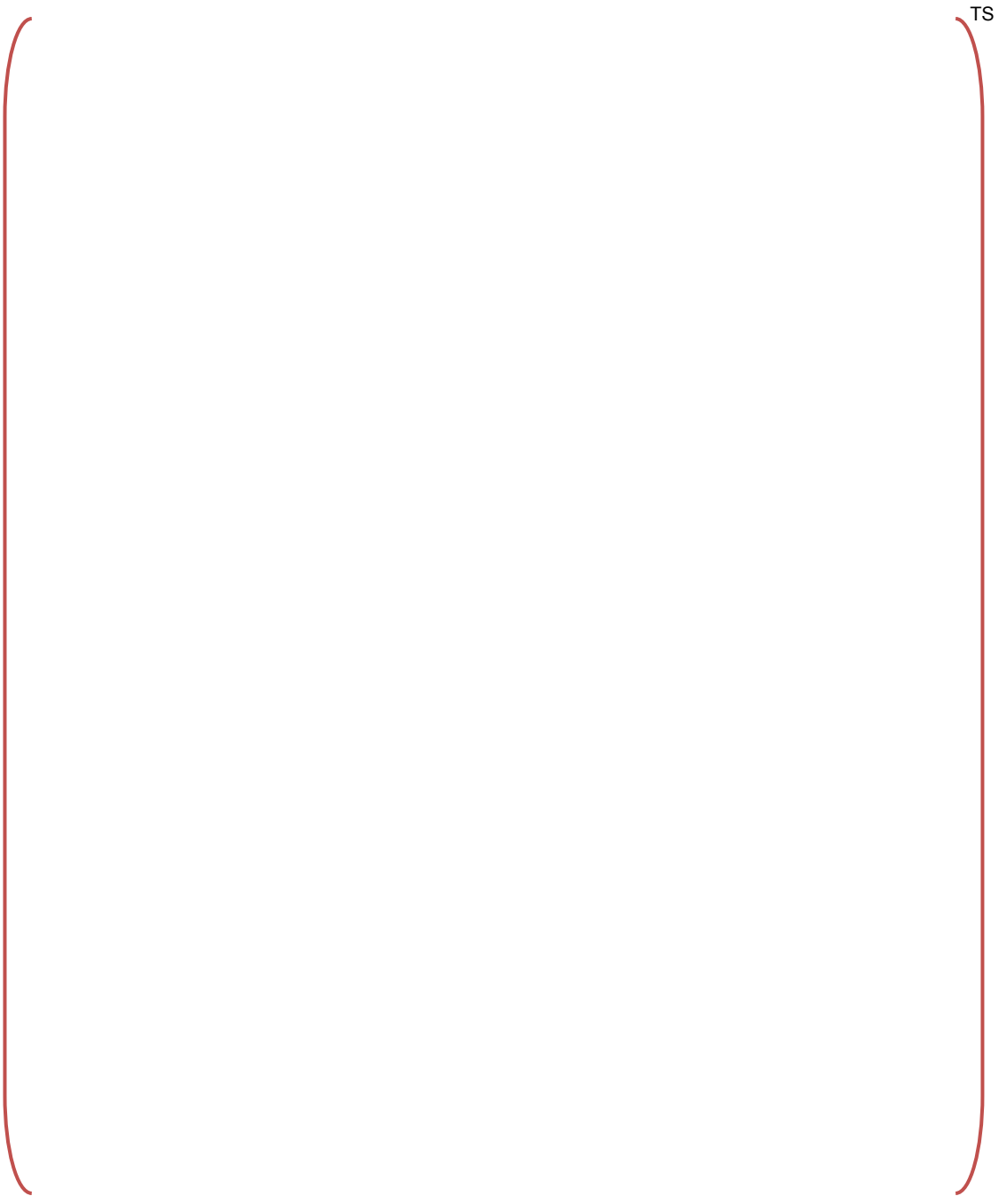

Figure 3.1-1 Drawing of the SIT (Side View)

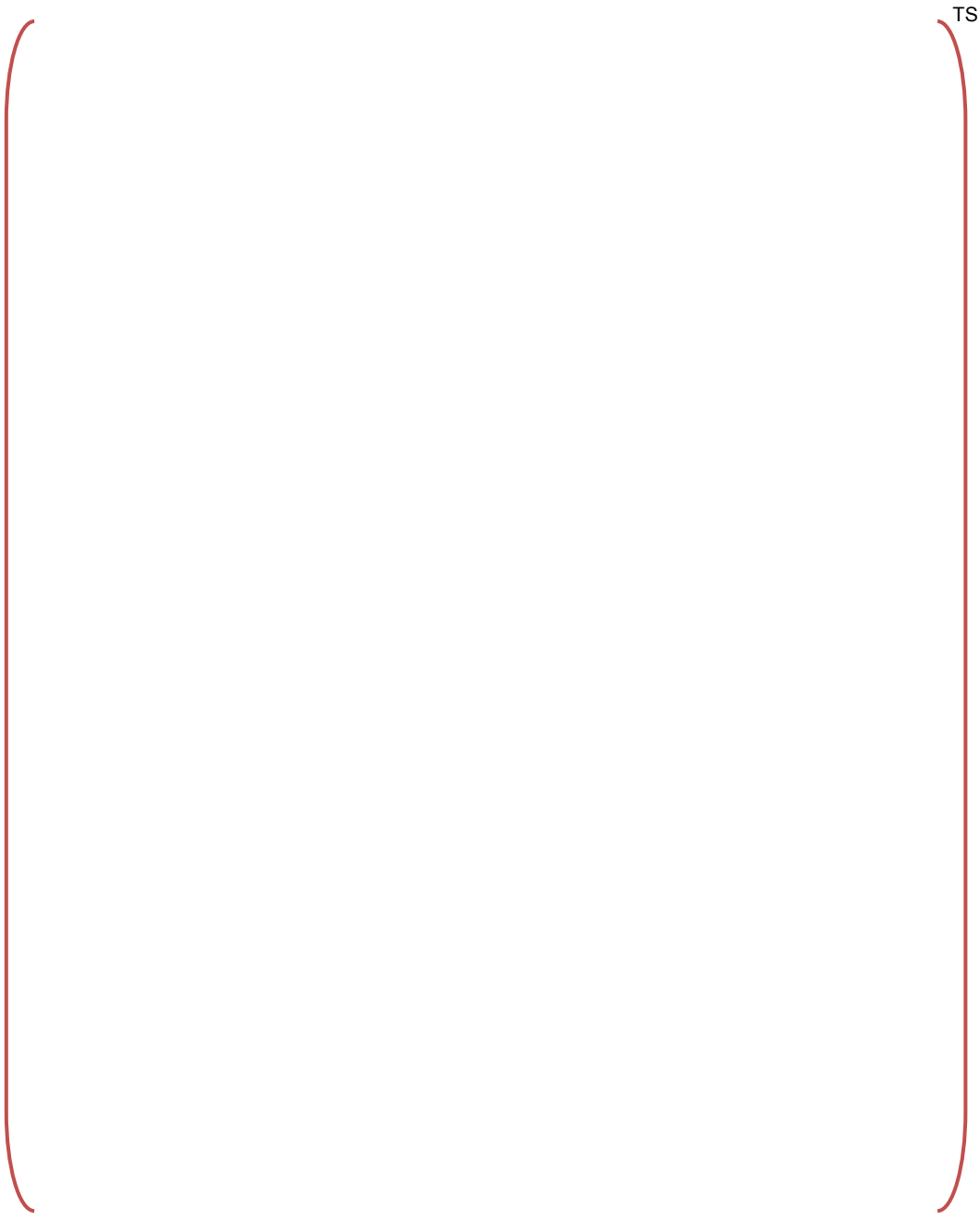

Figure 3.1-2 Drawing of the SIT (Top View)

3.2 Fluidic Device

A passive FD, which is installed in each of the SIT, provides two operational stages of safety water injection into the primary coolant system and results in more effective use of borated water in the SITs in the event of a LOCA. Once a LOCA occurs, the safety injection system with the FD initially delivers a large flow rate of safety injection water for a certain period of time, and thereafter, the flow rate is reduced to about [ ]^{TS} of the large flow rate.

The FD consists of the vortex chamber, main (supply) port, control port, and stand pipe (Fig. 3.1-1). The vortex chamber has the shape of a flat slice of cylinder and will be installed horizontally, with its axis overlapping the centerline of the SIT. The four supply nozzles and four control nozzles are connected in the 90 degrees symmetric manner to the vortex chamber. The stand pipe is connected to the supply port and its axis is overlapped with the centerline of the SIT. The time of flow switching is determined by the height of the stand pipe. The water flows through both supply and control ports when the water level is above the top of the stand pipe. In this case, the flow passage is almost straight and the flow resistance is minimal. On the other hand, when the water level is below the top of the stand pipe, the water flows only through the control ports. In this case, the flow experiences a high swirl before leaving the vortex chamber, which is a major reason of the high flow resistance and small flow rate.

The main dimensions of the APR1400 FD are summarized in Table 3.2-1. The size of the FD is the same as the FD used in the test except the height of stand pipe (See Table 4.1-1). The drawings of the FD are the same as those in the test facility shown in Appendix A.

The tests (Case-03 and Case-04) in Section 4.2 are the sensitivity tests to evaluate the effects of the manufacturing tolerances. These manufacturing tolerances are the expected maximum values for the APR1400 FD. Detailed test results are described in Section 4.2.

Table 3.2-1 Main Dimensions of the Fluidic Device

	TS
Outer Diameter of Fluidic Device	
Height of Fluidic Device	
Diameter of Vortex Chamber	
Height of Vortex Chamber	
Width of Supply Nozzle	
Width of Control Nozzle	
Angle between Neighboring Supply Nozzle and Control Nozzle	
Diameter of Exit Nozzle Throat	
Height of Stand Pipe	
Inner Diameter of Stand Pipe	

4. PERFORMANCE VERIFICATION TESTS

4.1 Test Facility

The performance of the APR1400 SIT-FD was evaluated and verified by using a full-scale test facility called VAPER. VAPER consists of the SIT, the FD, a compressed air supply system, a SIT water discharge pipe line, a SIT water supply & recirculation system, a stock tank and a data acquisition and control system as shown in Figure 4.1-1.

4.1.1 **Safety** Injection Tank

The SIT of the VAPER facility has an inner diameter of [ ]^{TS}, a height of [ ]^{TS}, and a volume of [ ]^{TS}, which has the same geometrical shape and size as the SIT of APR1400. The design pressure and temperature of the SIT are 5.0 MPa(a) (725 psia) and 90 ^{o}C (194 ^{o}F), respectively.

4.1.2 Fluidic Device

The FD of the VAPER facility has essentially the same geometrical shape and size as the FD of APR1400. The major dimensions of the FD are summarized in Table 4.1-1. The detailed drawings of the SIT and the FD of the VAPER facility are provided in Appendix A.

4.1.3 Subsidiary Components

The SIT is pressurized by compressed air instead of nitrogen gas. The maximum allowable pressure of the air-compressor is 5.0 MPa(a) (725 psia). The SIT pressurized by air will give a similar FD pressure loss coefficient as that pressurized by nitrogen, since the diffusion coefficients, kinematic viscosities and specific heat ratios of air and nitrogen are similar although the air has slightly higher solubility than nitrogen.

Unborated demineralized water is supplied to the SIT as SIT water. The water in the stock tank can be also supplied to the SIT by the recirculation pump.

The discharge pipe line at the downstream of the SIT has an inner diameter of [ ]^{TS}. A quick opening valve is installed in order to isolate the SIT while the SIT is being pressurized and to initiate the injection of SIT water. An orifice is installed to adjust the total pressure loss coefficient of the discharge pipe line.

The stock tank has a volume of 97 m^3 (3,426 ft^3), and the pressure of the tank is kept to be an atmospheric pressure condition during the experiments.

4.1.4 Measurement System

The initial water level and level change in the SIT are measured by a differential pressure transmitter. The pressure of the SIT and the temperature of the compressed air in the SIT are measured by a pressure transmitter and a thermocouple at the top of the SIT, respectively. The pressure drop across the FD is measured by a differential pressure transmitter. The level change in the stand pipe is measured by a differential pressure transmitter.

Pressure and differential pressure transmitters are model 3051C smart transmitters of Rosemount Inc., which were calibrated on site by a model 515 pressure controller/calibrator of Drug Ltd. An end-to-end calibration from the pressure transmitter to the data acquisition unit was carried out to minimize measurement errors related to the signal converters, isolators, and analog-to-digital converter as well as the measurement errors of the pressure and the differential pressure transmitters. The pressure controller/calibrator was calibrated at the Korea Research Institute of Standards and Science, at

less than [ ]^{TS} of the span at a 95% confidence level. The thermocouple was manufactured by Watlow Co., and has a sheath diameter of 0.25 mm (0.01 in). The analog-to-digital converter of the data acquisition unit has the 16 bit resolution for -10 to +10 Volt range.

Table 4.1-1 Main Dimensions of the VAPER Fluidic Device

	Case-01	Case-02	Case-03	Case-04 TS
Outer Diameter of Fluidic Device				
Height of Fluidic Device				
Diameter of Vortex Chamber				
Height of Vortex Chamber				
Width of Supply Nozzle				
Width of Control Nozzle				
Angle between Neighboring Supply Nozzle and Control Nozzle				
Diameter of Exit Nozzle Throat				
Height of Stand Pipe				
Inner Diameter of Stand Pipe				

Figure 4.1-1 Schematic of the VAPER Facility

4.2 Test Conditions

Four cases of tests were carried out to verify the performance of the VAPER SIT, the SIT installed in the VAPER facility. The reference test conditions are shown in Table 4.2-1 for each test case. Case-01 and Case-02 correspond to the standard FD tests. That is, the FD in Case-01 and Case-02 has almost the same geometrical dimensions as the FD of APR1400. But Case-02 has [ ]^{TS} higher stand pipe than Case-01 in order to examine the effect of stand pipe height on the FD performance.

Case-03 and Case-04 are sensitivity tests to evaluate the effects of the manufacturing tolerances. In Case-03, the height of the vortex chamber was reduced from [ ]^{TS}. In Case-04, the height of the vortex chamber was reduced from [ ]^{TS} and the width of the control nozzle was increased from [ ]^{TS}. These manufacturing tolerances are the expected maximum values for the APR1400 FD.

4.2.1 Case-01 Tests

Three identical tests were performed at the reference test condition in order to check the repeatability of the test results. One additional test was performed at about half of the reference pressure in order to evaluate the reliability of the pressure drop characteristics of the FD. The test conditions of Case-01 tests are summarized in Table 4.2-2.

4.2.2 Case-02, Case-03 and Case-04 Tests

In order to check the repeatability of the test results, three identical tests were performed at the reference test conditions for Case-02, Case-03 and Case-04 tests. The test conditions of Case-02, Case-03 and Case-04 are summarized in Tables 4.2-3, 4.2-4 and 4.2-5, respectively.

Table 4.2-1 Reference Test Conditions for the Performance Verification Tests of the VAPER SIT

	Case-01, -03, -04	Case-02
Initial SIT gas pressure		
Initial SIT water level		
SIT water volume above the top of stand pipe (volume for large flow)		
SIT water volume below the top of stand pipe (volume for small flow)		
Initial SIT water temperature		
Stock tank pressure		

TS

Table 4.2-2 Test Conditions of Case-01 Tests

Test ID	Initial SIT pressure [kPa(g) (psig)]	Initial SIT water level [m (ft)]	Initial SIT Temperature [°C (°F)]
Case-01-01			
Case-01-02			
Case-01-03			
Case-01-04			

TS

Table 4.2-3 Test Conditions of Case-02 Tests

Test ID	Initial SIT pressure [kPa(g) (psig)]	Initial SIT water level [m (ft)]	Initial SIT Temperature [°C (°F)]
Case-02-01			
Case-02-02			
Case-02-03			

TS

Table 4.2-4 Test Conditions of Case-03 Tests

Test ID	Initial SIT pressure [kPa(g) (psig)]	Initial SIT water level [m (ft)]	Initial SIT Temperature [°C (°F)]
Case-03-01			
Case-03-02			
Case-03-03			

TS

Table 4.2-5 Test Conditions of Case-04 Tests

Test ID	Initial SIT pressure [kPa(g) (psig)]	Initial SIT water level [m (ft)]	Initial SIT Temperature [°C (°F)]
Case-04-01			
Case-04-02			
Case-04-03			

TS

4.3 Test Results

The summary of the test results for Case-01, Case-02, Case-03 and Case-04 is provided in Table 4.3-1. Complete sets of the test results are provided in KAERI's report [1]. The repeatability of the test results was confirmed, and the effects of the stand pipe height and the manufacturing tolerances on the FD performance were insignificant. The pressure loss coefficient (K-factor) of the FD obtained from the low pressure test (Case-01-04) was similar to the pressure loss coefficient obtained from the reference pressure tests. The results show that the pressure loss coefficient of the FD has little or no dependence on the pressure difference between the SIT and the reactor coolant system as well as the initial SIT pressure. Details of the test results are described in the following sections.

4.3.1 Water Levels in the SIT and Stand Pipe

The level changes in the SIT and the stand pipe are shown in Figure 4.3-1 for Case-01 tests, and comparisons are made among Case-01, Case-02, Case-03, and Case-04 tests in Figure 4.3-2. The base elevation of the SIT water level is the bottom of the SIT, and the base elevation of the stand pipe water level is [ ]^{TS} higher than the top surface of the FD. As a result, the base elevation of the stand pipe water level is [ ]^{TS} higher than that of the SIT water level.

The water level of the SIT decreased steeply until the water level reached the top of the stand pipe, then the water level gradually decreased. When the water level of the SIT dropped below the top of the stand pipe, the water level in the stand pipe was depressed abruptly and reached the lowest level, and then recovered rapidly to about a [ ]^{TS} elevation, thereafter the water level slowly decreased.

There was no flow path through the supply port after the water level dropped below the top of the stand pipe, and the pressure drop occurred only through the control ports. The water level inside the stand pipe was lowered to compensate for pressure drop and to balance the pressure difference between the vortex chamber and the top of the SIT. The stand pipe water level reached the minimum level at the time of the abrupt depression due to inertia effect.

4.3.2 SIT Water Injection Flow Rate

The injection flow rate of the SIT water was deduced from the decreasing rate of SIT water level as follows:

$$W_{SI}(t) = -\rho_{wtr} A_{SIT} \frac{dh_{SIT}(t)}{dt} \cong \rho_{wtr} A_{SIT} \frac{h_{SIT}(t) - h_{SIT}(t+\Delta t)}{\Delta t} \quad (4.3\text{-}1)$$

where W_{SI} : injection flow rate of the SIT water (kg/sec),

ρ_{wtr} : density of SIT water (kg/m^3),

A_{SIT} : cross-sectional area of the SIT (m^2),

Δt : time difference (seconds).

The SIT water level decreased almost linearly with time (Figures 4.3-1 ~ 4.3-2). The instantaneous change rate of water level at time t could be approximated by first order differentiation (Eq. (4.3-1)) without causing a significant error in the evaluation of the injection flow rate. The injection flow rate was calculated with a time difference of [ ]^{TS}. However, the injection flow rate calculated by Eq. (4.3-1) might deviate from the actual flow rate when the decrease rate of the SIT water level is not linear such as the initial SIT water injection period and the flow rate turning period.

The injection characteristics of the VAPER SIT are shown in Figure 4.3-3 for Case-01 tests, and comparisons are made among Case-01, Case-02, Case-03, and Case-04 tests in Figure 4.3-4. The injection flow rate decreased rapidly when the water level in the SIT dropped below the top of the stand pipe. The peak injection flow rate was about [ ]^{TS}. The injection flow rate after the flow rate turning point was less than [ ]^{TS}. The total duration of the injection was [ ]^{TS}.

4.3.3 Pressure Loss Coefficient of the Fluidic Device

The pressure loss coefficient of the FD (FD K-factor) was determined based on the pressure drop across the FD as follows:

$$K_{FD} = \Delta P_{FD} \frac{2}{\rho_{wtr} U_{SI}^2} = \Delta P_{FD} \frac{2\rho_{wtr} A_{Pipe}^2}{W_{SI}^2} \qquad (4.3\text{-}2)$$

where K_{FD} : pressure loss coefficient of the FD,

ΔP_{FD} : pressure drop across the FD (Pa),

U_{SI} : area averaged velocity of SIT water (m/sec),

A_{Pipe} : cross-sectional area of the SIT discharge line of APR1400 (m^2).

The pressure loss coefficient of the FD is shown in Figure 4.3-5 for Case-01 tests, and comparisons are made among Case-01, Case-02, Case-03, and Case-04 tests in Figure 4.3-6. Table 4.3-1 shows the time averaged pressure loss coefficient of the FD for both large and small flow rate periods. Generally, the average value was taken for about [ ]^{TS} period for the large flow rate condition, and for about [ ]^{TS} period for the small flow rate condition. However, the exact time period is slightly different among the test cases.

The time averaged pressure loss coefficient of the FD was [ ]^{TS} for the large flow rate period before the flow rate turning point, and about [ ]^{TS} for the small flow rate period. Almost a [ ]^{TS} higher pressure loss coefficient was achieved for the small flow rate period compared to the large flow rate period due to the swirling motion inside the vortex chamber.

In the postulated LBLOCA, the RCS pressure is much higher than the atmospheric pressure during the initial operation period of the APR1400 SIT. Contrary to the varying RCS pressure condition, VAPER tests were performed at the constant back pressure condition which was kept atmospheric. However, as indicated in Table 4.3-1, Case-01-04 test showed that the pressure loss coefficient of the FD was not dependent on the pressure difference between the SIT and the reactor coolant system. Moreover, the effect of absolute pressure change on the physical properties of SIT water is negligible. Therefore, it can be concluded that the varying RCS pressure, which is higher than the atmospheric pressure, has little effect on the pressure loss coefficient of the FD.

4.3.4 Air Discharge Characteristics of the SIT

As can be seen in Figures 4.3-1 and 4.3-2, the water level in the stand pipe after the SIT level decreased below the top of the stand pipe was always lower than the water level in the SIT. As a result, the water in the stand pipe became depleted before the water in the SIT was completely discharged. Then, the air in the upper part of the SIT could be discharged through the empty stand pipe. The inception of this air discharge was evaluated in the VAPER SIT performance verification tests.

The volume expansion of the air due to the level change in the SIT can be approximated as the following, if a polytropic expansion is assumed and the total air mass is conserved:

$$\left(PV^n\right)_{air,0} = \left(PV^n\right)_{air,t} = \left(PV^n\right)_{air,t+\Delta t} \qquad (4.3\text{-}3)$$

Where P : pressure of air in the upper part of the SIT (Pa),

V : volume of air in the upper part of the SIT (m^3),

n : index of polytropic process,

0 : initial time of the SIT water discharge.

The injection flow rate of the SIT water can be also evaluated from the volume expansion rate of the air and using Eq. (4.3-3) as follows:

$$W_{SI}(t) = \rho_{wtr} \cdot \left(\frac{dV}{dt}\right)_{air,t} \cong \rho_{wtr} \frac{V_{air,t+\Delta t} - V_{air,t}}{\Delta t} = \rho_{wtr} \cdot \left(P^{1/n} \cdot V\right)_{air,t} \cdot \frac{1}{\Delta t}\left[\left(\frac{1}{P}\right)^{1/n}_{air,t+\Delta t} - \left(\frac{1}{P}\right)^{1/n}_{air,t}\right] \quad (4.3\text{-}4)$$

The injection flow rates of the SIT water by Eqs. (4.3-1) and (4.3-4) are shown in Figures 4.3-7 ~ 4.3-10 for Case-01, Case-02, Case-03 and Case-04 tests, respectively. The injection flow rate was calculated with a time difference of [ ]^{TS}.

The index of the polytropic process has different values depending on the type of expansion process. The SIT water injection flow rate by Eq. (4.3-4) well matched the injection flow rate by Eq. (4.3-1) when the index of the polytropic process was [ ]^{TS} for the large flow and small flow periods, respectively. As can be seen in Fig. 4.3-11, the air temperature dropped very steeply during the large flow period while the air temperature remained more or less constant during the small flow period. Therefore, it is reasonable that the index of the polytropic process has different values of [ ]^{TS} for the large flow and small flow periods, respectively.

The injection flow rates by Eqs. (4.3-1) and (4.3-4) agreed well with each other until the time of about [ ]^{TS}. However, the injection flow rate calculated by Eq. (4.3-4) increased very steeply from about [ ]^{TS} because the air started to be discharged from the SIT through the empty stand pipe and the total air mass was no longer conserved.

Figures 4.3-7 ~ 4.3-10 show the inception of the air discharge started at about [ ]^{TS} in VAPER SIT performance tests. Owing to the higher stand pipe in the Case-02 tests, the inception of the air discharge was delayed about [ ]^{TS} compared with the Case-01, which corresponds to the inception time of about [ ]^{TS}.

The discharge flow rate of the air is also evaluated from the total air mass change rate as follows:

$$W_{air}(t) = \frac{m_{air}(t) - m_{air}(t+\Delta t)}{\Delta t} \quad (4.3\text{-}5)$$

$$m_{air}(t) = \rho_{air}(t) \cdot V_{air}(t) \quad (4.3\text{-}6)$$

The air volume was calculated by subtracting the SIT water volume from the total SIT volume. The air density was determined by the measured pressure and temperature of the air along with an ideal gas law as follows:

$$\rho_{air}(t) = \frac{P_{air}(t)}{R \cdot T_{air}(t)} \quad (4.3\text{-}7)$$

For Case-01 tests, the discharge flow rate of the air showed the first peak of about [ ]^{TS} at the time of around [ ]^{TS}, and reached the maximum of about [ ]^{TS} when the SIT water was totally depleted (Figures 4.3-12).

The volumetric discharge flow rate of the air was obtained by dividing the mass flow rate of the air by the air density and it is shown in Figure 4.3-13 for Case-01-01 test. The air density was calculated by the pressure and temperature measured at the top part of the SIT. After the inception at around [ ]^{TS}, the volumetric discharge flow rate increased steadily until about [ ]^{TS}. Thereafter, it was more or less constant until about [ ]^{TS} at which the SIT water was totally depleted.

The FD K-factor of Case-01-01 test at the small flow condition was evaluated for [ ]^{TS} period, which included the early phase of air discharge [ ]^{TS} shown in Figures 4.3-12 and 4.3-13. The FD K-factor averaged over the period of [ ]^{TS} was [ ]^{TS} as shown in Table 4.3-1. The FD K-factors averaged over the periods of [ ]^{TS} and [ ]^{TS} were [ ]^{TS} and [ ]^{TS}, respectively. This implies that the difference among the three FD K-factors averaged over different time periods would be due to the random unsteadiness of the swirling flow inside the vortex chamber of the FD, and the FD K-factor was not sensitive to the amount of air discharge flow rate for the period of [ ]^{TS}.

Table 4.3-1 Summary of the Test Results (Case-01, Case-02, Case-03, Case-04)

Test ID	Peak flow rate [kg/sec (lb/sec)]	Duration of injection [sec]	Fluidic Device K-factor Note1
Case-01-01			
Case-01-02			
Case-01-03			
Case-01-04 Note2			
Case-02-01			
Case-02-02			
Case-02-03			
Case-03-01			
Case-03-02			
Case-03-03			
Case-04-01			
Case-04-02			
Case-04-03			

TS

Note 1: Large flow / small flow condition

Note 2: Low pressure condition

Figure 4.3-1 Level Changes in the SIT and the Stand Pipe (Case-01 Tests)

Figure 4.3-2 Comparison of Level Changes in the SIT and the Stand Pipe (Case-01~04 Tests)

Figure 4.3-3 Injection Flow Rate of SIT Water from the VAPER SIT (Case-01 Tests)

Figure 4.3-4 Comparison of Injection Flow Rate of the SIT Water (Case-01~04 Tests)

Figure 4.3-5 Pressure Loss Coefficient (K-factor) of the Fluidic Device (Case-01 Tests)

Figure 4.3-6 Comparison of the K-factor of the Fluidic Device (Case-01~04 Tests)

Figure 4.3-7 Inception of Air Discharge from the VAPER SIT (Case-01-01 Test)

Figure 4.3-8 Inception of Air Discharge from the VAPER SIT (Case-02-01 Test)

Figure 4.3-9 Inception of Air Discharge from the VAPER SIT (Case-03-01 Test)

Figure 4.3-10 Inception of Air Discharge from the VAPER SIT (Case-04-01 Test)

Figure 4.3-11 Variation of Air Temperature in the Upper Region of the VAPER SIT (Case-01-01 Test)

Figure 4.3-12 Mass Flow Rate of Discharged Air from the VAPER SIT (Case-01-01 Test)

Figure 4.3-13 Volumetric Flow Rate of Discharged Air from the VAPER SIT (Case-01-01 Test)

4.4 Uncertainty Evaluation

The uncertainties of the pressure loss coefficient (K-factor) of the FD were analyzed at a 95% confidence level in accordance with the guidelines of ISO [2] and ANSI/ASME [3]. As shown in Eq. (4.4-1), the systematic uncertainty of the SIT water injection flow rate was evaluated through a propagation of the elemental uncertainty sources in Eq. (4.3-1) as follows:

$$B_{W_{SI}} = \pm\left[\left(\frac{\partial W_{SI}}{\partial \rho_{wtr}} B_{\rho_{wtr}}\right)^2 + \left(\frac{\partial W_{SI}}{\partial A_{SIT}} B_{A_{SIT}}\right)^2 + \left(\frac{\partial W_{SI}}{\partial \Delta h_{SIT}} B_{\Delta h_{SIT}}\right)^2\right]^{1/2}$$
$$= \pm\left[\left(\frac{W_{SI}}{\rho_{wtr}} B_{\rho_{wtr}}\right)^2 + \left(\frac{W_{SI}}{A_{SIT}} B_{A_{SIT}}\right)^2 + \left(\frac{W_{SI}}{h_{SIT}(t) - h_{SIT}(t+\Delta t)} B_{\Delta h_{SIT}}\right)^2\right]^{1/2} \quad (4.4\text{-}1)$$

The elemental parameters had the following systematic uncertainties: a water density of [ ]^{TS}; a SIT cross-sectional area of [ ]^{TS}; and a SIT level change for Δt seconds of [ ]^{TS}. The estimated systematic uncertainty of the injection flow rate was [ ]^{TS} for the large flow rate period and [ ]^{TS} for the small flow rate period, as shown in Figure 4.4-1. The uncertainty related with Δt was neglected.

The systematic uncertainty of the pressure loss coefficient of the FD was also evaluated through a propagation of the elemental uncertainty sources in Eq. (4.3-2) as follows:

$$B_K = \pm\left[\left(\frac{\partial K}{\partial \Delta P} B_{\Delta P}\right)^2 + \left(\frac{\partial K}{\partial \rho_{wtr}} B_{\rho_{wtr}}\right)^2 + \left(\frac{\partial K}{\partial A_{Pipe}} B_{A_{Pipe}}\right)^2 + \left(\frac{\partial K}{\partial W_{SI}} B_{W_{SI}}\right)^2\right]^{1/2}$$
$$= \pm\left[\left(\frac{K}{\Delta P} B_{\Delta P}\right)^2 + \left(\frac{K}{\rho_{wtr}} B_{\rho_{wtr}}\right)^2 + \left(2\frac{K}{A_{Pipe}} B_{A_{Pipe}}\right)^2 + \left(2\frac{K}{W_{SI}} B_{W_{SI}}\right)^2\right]^{1/2} \quad (4.4\text{-}2)$$

The elemental parameters had the following systematic uncertainties: SIT water injection flow rate of [ ]^{TS} and [ ]^{TS} for the large and small flow rate periods, respectively; a piping cross-sectional area of ± 1 %; and a pressure drop across the FD of [ ]^{TS}. The estimated systematic uncertainty of the pressure loss coefficient of the FD was [ ]^{TS} for the large flow period and [ ]^{TS} for the small flow rate periods with an average of [ ]^{TS}, as shown in Figure 4.4-2.

The random uncertainty of the pressure loss coefficient of the FD was evaluated from a multiplication of the standard deviation of the pressure loss coefficient in Table 4.3-1 and the coverage factor of the student *t*-distribution with a degree of freedom of 12 as follows:

$$P_K = \pm t_{95} S_{\bar{K}} \quad (4.4\text{-}3)$$

The standard deviation was [ ]^{TS} and [ ]^{TS} for the large and small flow rate periods, respectively, and the coverage factor was [ ]^{TS}. The estimated random uncertainty of the pressure loss coefficient was [ ]^{TS} and [ ]^{TS} for the large and small flow rate periods, respectively. This random uncertainty reflected the effects of the process unsteadiness, the differences in the test conditions, and the manufacturing tolerances. Finally, the total uncertainty of the pressure loss coefficient of the FD was estimated by the root sum square of the systematic and random uncertainties as follows:

$$U_{95} = \pm\left(B_K^2 + P_K^2\right)^{1/2} \quad (4.4\text{-}4)$$

The total uncertainty of the pressure loss coefficient of the FD is shown in Figure 4.4-3 and the average was [ ]^{TS} and [ ]^{TS} for the large and small flow rate periods, respectively.

Figure 4.4-1 Systematic Uncertainty of the Injection Flow Rate of the SIT Water

Figure 4.4-2 Systematic Uncertainty of the Fluidic Device K-factor

Figure 4.4-3 Total Uncertainty of the Fluidic Device K-factor

4.5 Quality Assurance Program

4.5.1 General

The Quality Assurance (QA) Program [4,5] for the 'Fluidic Device Performance Verification Tests (FD Tests)' was developed in accordance with 10CFR50 Appendix B and ANSI/ASME NQA-1-1994. This QA Program covers the QA requirements that are applicable to experimental test activities.

4.5.2 Test Equipment

Control of test and measuring equipment was carried out in accordance with the established procedure. The test team has generated and maintained QA records such as Measuring & Test Equipment (M&TE) List, M&TE History Cards, and Calibration Reports.

4.5.3 Test Personnel

The FD Tests were conducted by competent and trained personnel. All test personnel received a high level of education, and had expertise and experiences in testing in thermal hydraulic experiments through performing R&D projects sponsored by the Korean Government, etc.

4.5.4 Test Procedure

The FD Tests were conducted in accordance with the documented procedure which had been issued after the review of QA personnel. The VAPER test facility was also operated in accordance with the established procedure. The Test Procedure [6], "FD-EP-01, Procedure for FD Performance Verification Tests," was developed for the FD Tests.

The Test Procedure includes test objectives and requires provisions for assuring that prerequisites has been met, that adequate instrumentation is available and used, and that suitable environmental condition is maintained. The required test items for APR1400 were accurately identified and tested in accordance with the Test Procedure.

Each test process was checked with documented check-list in accordance with the Test Procedure. QA personnel also witnessed the selected points for some representative tests.

4.6 Summary of Performance Verification Tests

A series of tests were carried out to verify the performance of the SIT-FD using the VAPER test facility. It was demonstrated that the SIT-FD can passively control the injection flow rate of SIT water without any moving part or any action of the plant operator with the help of the FD. The VAPER SIT showed sufficient repeatability with regard to its performance, and the pressure loss coefficient of the FD is not materially affected by (1) the initial SIT pressure, (2) the height of the stand pipe, and (3) the expected manufacturing tolerances.

For the large flow injection period, the average of the pressure loss coefficient of the FD is [ ]^{TS}, and the total uncertainty of the pressure loss coefficient is [ ]^{TS}. That is, the pressure loss coefficient of the FD would be in the range of [ ]^{TS}, which satisfies the design requirement of [ ]^{TS} for the pressure loss coefficient of the FD in the large flow injection period.

For the small flow injection period, the average of the pressure loss coefficient of the FD is [ ]^{TS}, and the total uncertainty of the pressure loss coefficient is [ ]^{TS}. That is, the pressure loss coefficient of the FD would be in the range of ^{TS}, which satisfies the design requirement of [ ]^{TS} for the pressure loss coefficient of the FD in the small flow injection period.

As a result, the SIT-FD will meet the design requirements with sufficient margin for both the large and small flow injection periods.

5. APPLICABILITY

5.1 Representative Pipe Area for the Fluidic Device K-Factor

The pressure loss coefficient of vortex devices are often evaluated using the exit nozzle diameter shown in Figure A-4. With regard to the LBLOCA analysis using a thermal hydraulic system analysis code such as RELAP5, the injection flow rate of SIT water is calculated based on the total pressure loss coefficient of the SIT discharge line and the FD as presented in Eq. (5.1-1). In this case, it is more convenient to use the same representative pipe area for the pressure loss coefficients of both the SIT discharge line and the FD. The pipe area of the SIT discharge line has been used as the representative pipe area.

$$\begin{aligned} K_{SI,Total} &= K_{SI,Pipe} + K_{FD} \\ &= \left(\Delta P_{SI,Pipe} + \Delta P_{FD}\right)\frac{2}{\rho_{wtr} U_{SI}^2} \\ &= \left(\Delta P_{SI,Pipe} + \Delta P_{FD}\right)\frac{2\rho_{wtr} A_{pipe}^2}{W_{SI}^2} \end{aligned} \qquad (5.1\text{-}1)$$

where $K_{SI,Total}$: total pressure loss coefficient of the SIT discharge line and the FD,

$K_{SI,Pipe}$: pressure loss coefficient of the SIT discharge line,

$\Delta P_{SI,Pipe}$: pressure drop across the SIT discharge line (Pa).

The diameter of the discharge pipe line [ ]^{TS} of the VAPER test facility (shown in Figure 4.1-1) is different from the diameter of the SI discharge line [ ]^{TS} of APR1400. However, the pressure drop across the FD is mostly affected by the detailed configuration of the vortex chamber, not by the diameter of the discharge pipe line. Therefore, the pressure loss coefficient of the FD in the VAPER facility was evaluated using the cross-sectional area of the SIT discharge line of APR1400 as the representative pipe area.

5.2 Effect of Dissolved Nitrogen Gas on the Fluidic Device K-Factor

In the case of VAPER tests, the SIT was pressurized by compressed air from atmospheric pressure to about [ ]^{TS} for several hours. On the other hand, the SIT in an actual plant is kept pressurized at about [ ]^{TS} by nitrogen gas for much longer time than the VAPER tests. As a result, the SIT water in the actual plant has higher solubility of nitrogen gas than the VAPER tests. Some of the dissolved nitrogen gas would come out of the SIT water when the SIT water passes through the throat (or the exit nozzle) of the FD where the pressure drops to the minimum value. In this section, the amount of the nitrogen gas coming out of the SIT water and its effect on the FD K-factor are roughly estimated.

The solubility of nitrogen gas in SIT water was calculated by a curve fitting the values in Tables 5.2-1 and 5.2-2 provided by Sun et al. [7]. The curve fitted equations for the mass of dissolved nitrogen gas per unit mass of SIT water are

$$m_{N_2}(P) = -1.37578\times10^{-6} + 2.84063\times10^{-4}\cdot P - 5.04235\times10^{-6}\cdot P^2 \qquad (5.2\text{-}1)$$

for SIT water at 0 ^{o}C (32^{o}F), and

$$m_{N_2}(P) = -1.23253\times10^{-6} + 1.54337\times10^{-4}\cdot P - 1.90901\times10^{-6}\cdot P^2 \qquad (5.2\text{-}2)$$

for SIT water at 40 ^{o}C (104^{o}F), and $m_{N_2}(P)$ is kg of nitrogen gas per kg of SIT water, P is MPa. In Eqs. (5.2-1) and (5.2-2), the effect of boron in SIT water on the solubility was ignored.

The nitrogen gas release rate (kg/sec) was calculated using Equation (5.2-3) by assuming that the nitrogen gas content in the SIT water reaches the equilibrium state of the solubility given in Tables 5.2-1 and 5.2-2 during the fast pressure transient process across the FD,

$$W_{N_2} = \left[m_{N_2}\left(P_{FD,in}\right) - m_{N_2}\left(P_{FD,throat}\right) \right] W_{SI} \quad (5.2\text{-}3)$$

Where $P_{FD,in}$ is the pressure of the SIT water at the top surface of the FD, $P_{FD,throat}$ is the pressure of the SIT water at the throat (or exit nozzle) of the FD where the pressure is minimum, and W_{SI} is the injection flow rate of the SIT water (kg/sec). The pressure of the SIT water at the throat of the FD was calculated as follows:

$$P_{FD,throat} = P_{FD,in} - \Delta P_{FD} + \frac{\rho_{wtr}}{2}\left(U_{SI,FD,out}^2 - U_{SI,throat}^2 \right) \quad (5.2\text{-}4)$$

where $U_{SI,FD,out}$ and $U_{SI,throat}$ denote the velocities of SIT water at the discharge pipe and the throat of the FD, respectively, and the pressure of the SIT water at the top surface of the FD was calculated by adding the hydrostatic pressure to the measured SIT pressure at the top of the SIT.

Figure 5.2-1 shows the mass release rate (or flow rate) of nitrogen gas at the SIT water temperature of 0 ^{o}C (32^{o}F) and 40 ^{o}C (104^{o}F). The pressures of the SIT water at the inlet and the throat of the FD and the SIT water velocities at the outlet and the throat were calculated from the measured data of Case-01-01 test even though the SIT pressure and SIT water injection flow rate would be slightly different when the type of pressurizing gas and the SIT water temperature are changed from those used in the VAPER test. The mass release rate of nitrogen gas at the large flow rate period was higher than that at the small flow rate period. Lower SIT water temperature condition yielded higher mass release rate of nitrogen gas. Figure 5.2-2 shows the volumetric release rate (or flow rate) of nitrogen gas, where the nitrogen density was evaluated using the ideal gas law with the calculated pressure at the throat and the given SIT water temperature. The maximum mass and volumetric flow rate of nitrogen gas in Figures 5.2-1 and 5.2-2 are much smaller than the air discharge flow rate during the period of [ ]^{TS} in Figures 4.3-12 and 4.3-13. As a result, the evolution of dissolved nitrogen gas does not matrially affect the FD K-factor.

Table 5.2-1 N_2 Solubility (kg/kg_{water}) in Pure Water at 0 °C (32 °F)

P [MPa(a) (psia)]	Solubility (kg/kg_{water})	
	Sun et al. [7]	Eq. 5.2-1
0.1 (14.5)		
0.5 (72.5)		
1.0 (145)		
2.5 (363)		
5.0 (725)		

TS

Table 5.2-2 N_2 Solubility (kg/kg_{water}) in Pure Water at 40 °C (104 °F)

P [MPa(a) (psia)]	Solubility (kg/kg_{water})	
	Sun et al. [7]	Eq. 5.2-2
0.1 (14.5)		
0.5 (72.5)		
1.0 (145)		
2.5 (363)		
5.0 (725)		

TS

Figure 5.2-1 Expected Mass Release Rate (or Flow Rate) of Nitrogen Gas for the Operating Condition Equivalent to Case-01-01 at Two Different SIT Water Temperatures

Figure 5.2-2 Expected Volumetric Release Rate (or Flow Rate) of Nitrogen Gas for the Operating Condition Equivalent to Case-01-01 at Two Different SIT Water Temperatures

6. SUMMARY

To improve the effectiveness of SIT water and to simplify the SIS, a passive flow controlling FD has been developed and installed inside the SIT for APR1400. The SIT-FD can passively control the injection flow rate of SIT water without any moving part or any action of the plant operator with the help of the FD. When the SIT water level is high and above the top of the stand pipe, water enters the vortex chamber through both the supply port and the control ports and thus it injects water at a large flow rate. When the water level drops below the top of the stand pipe, the water enters the vortex chamber only through the control ports and thus vortex formation in the vortex chamber achieves the small flow injection.

The performance of the passive SIT-FD was evaluated in the VAPER test facility, equipped with a prototypical full-scale SIT. The repetitive tests verify that the performance of the SIT-FD satisfies the design requirements of the SIT-FD and the reproducibility of the SIT-FD has been confirmed. The pressure loss coefficient of the small flow rate period is almost [ ]^{TS} larger than that of the large flow rate period due to the strong vortex motion in the FD.

In addition, the implementation of a quality assurance program for the FD tests assures the high quality of the experimental results.

REFERENCES

[1] Data Base of Fluidic Device Performance Verification Experiment, KAERI/THETA-FD2, Rev.1 (2012).

[2] ISO, Guide to the Expression of Uncertainty in Measurement, ISBN 92-67-10188-9 (1995).

[3] ASME, Test Uncertainty, ASME PTC 19.1-1998 (1998).

[4] Quality Assurance Manual, APR1400 Fluidic Device Verification Experiment (2003).

[5] Quality Assurance Procedures, APR1400 Fluidic Device Verification Experiment (2003).

[6] FD Performance Repeatability Experimental Procedure, FD-EP-01 (2004).

[7] R. Sun, W. Hu, Z. Duan, "Prediction of Nitrogen Solubility in Pure Water and Aqueous NaCl Solutions up to High Temperature, Pressure, and Ionic Strength," Journal of Solution Chemistry, Vol. 30, No. 6, pp. 561-573 (2001).

Appendix A Drawing of the SIT and Fluidic Device of the VAPER Facility

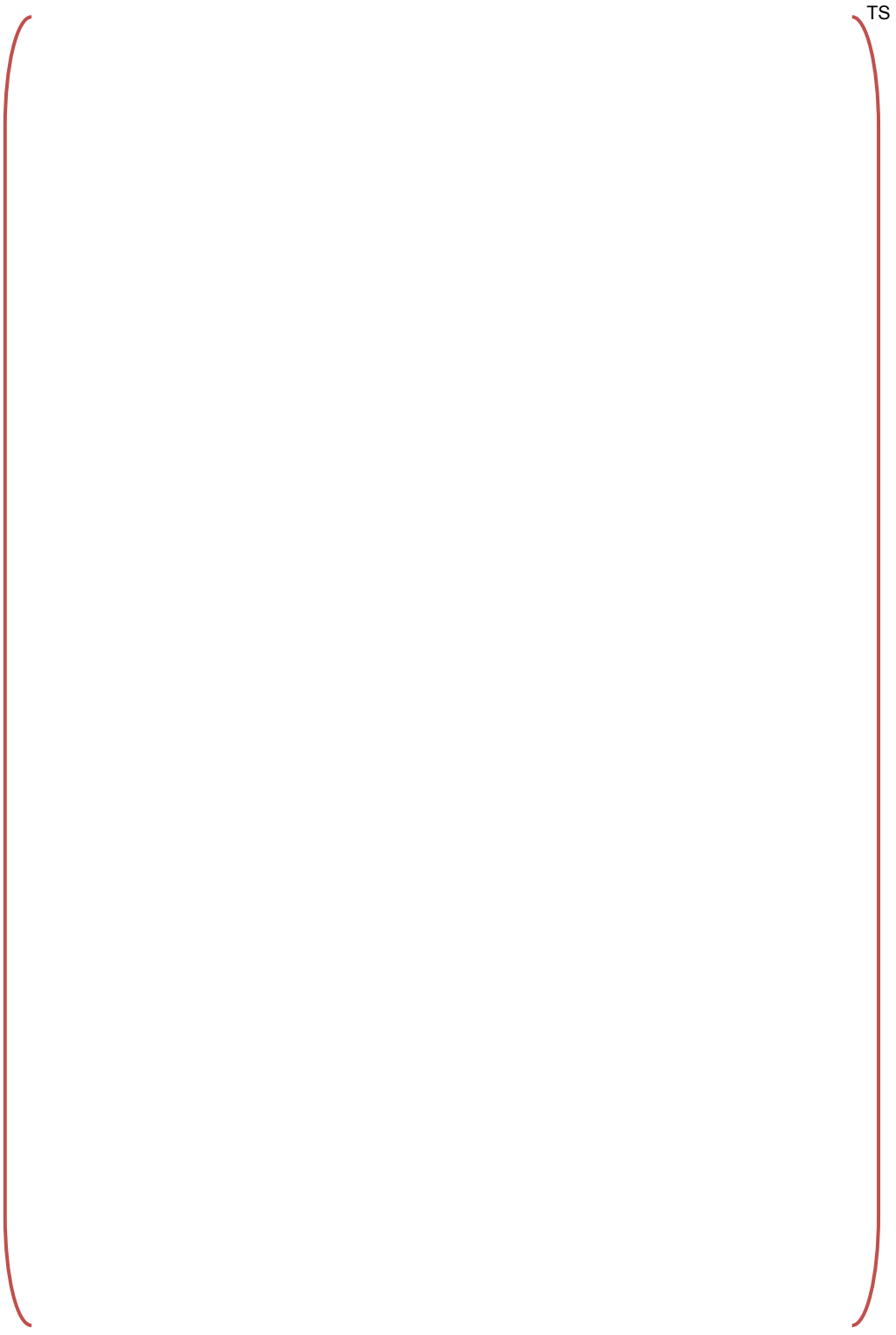

Figure A-1 Drawing of the VAPER SIT

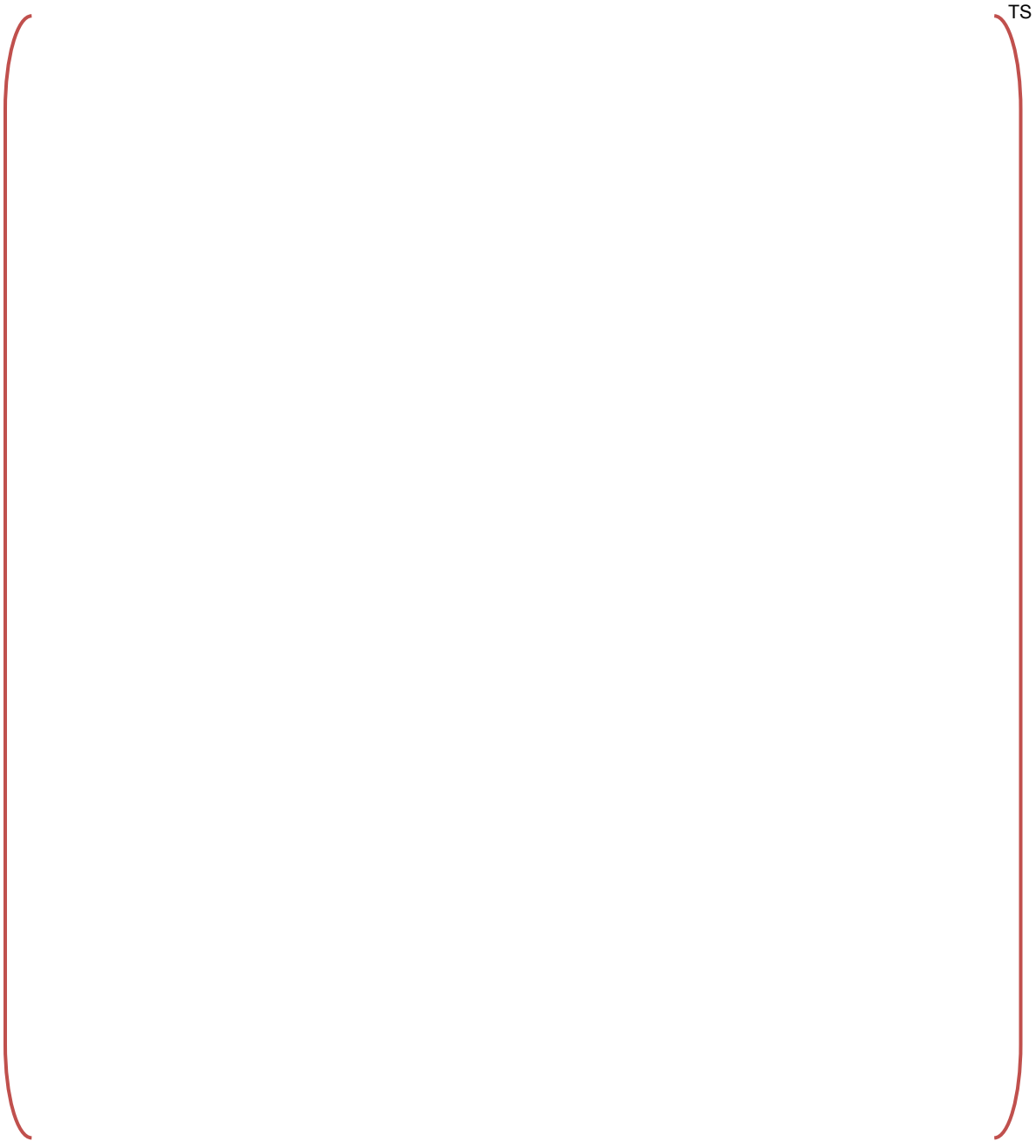

Figure A-2 Drawing of the VAPER SIT and the Fluidic Device

Figure A-3 Drawing of the Insert Plates in the Vortex Chamber

TS

Figure A-4 Drawing of the Exit Nozzle in the Vortex Chamber

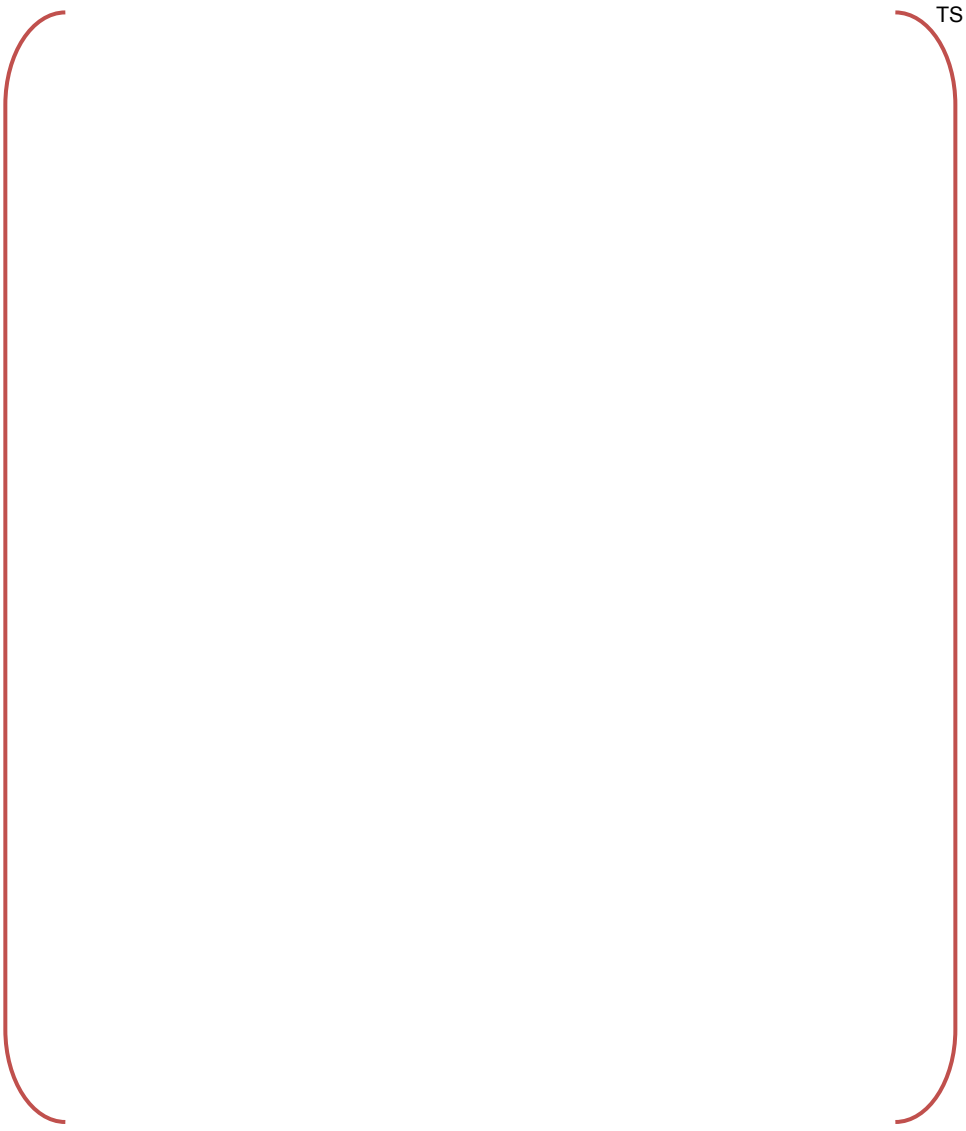

Figure A-5 Drawing of the Discharge Pipe connected to the Exit Nozzle

Page intentionally left blank

SECTION C

Page intentionally left blank

Non-Proprietary

KHNP
KOREA HYDRO & NUCLEAR POWER CO., LTD
70-1312-gil, Yuseong-daero, Yuseong-gu, Daejeon, 305-343, KOREA
Tel: +82-42-870-5740 / Fax: +82-42-870-5779
http://www.khnp.co.kr

April 11, 2014
Document Control Desk
U.S. Nuclear Regulatory Commission
Washington, DC 20555-0001

Attention: Mr. Jeffrey Ciocco
Division of New Reactor Licensing

Project No.0782
MKD/NW-14-0008L

Subject: Submittal of KHNP Responses to Request for Additional Information 2-7371

Reference: 1) NRC Request for Additional Information 2-7371, dated March 11, 2014 (NRC Project 0782)
2) KHNP Topical Report: Fluidic Device Design for the APR1400, Revision 0, December 2012 (APR1400-Z-M-TR-12003)

KHNP is hereby submitting responses to the Request for Additional Information (RAI) 2-7371, dated March 11, 2014. The RAI and responses are related to KHNP's Topical Report, APR1400-Z-M-TR-12003 (R0).

Enclosure 1 contains one copy of the associated affidavit. Enclosure 2 provides "KHNP Responses to Request for Additional Information No. 2-7371" (Proprietary), and Enclosure 3 provides "KHNP Responses to Request for Additional Information No. 2-7371" (Non-proprietary).

If additional information or clarification is required, please contact Yun-ho Kim, Director of KHNP Washington DC Center at yunhokim@khnp.co.kr or 703-388-0592.

Sincerely,

M. K. Kim

Myung-Ki Kim
Project Manager
Advanced Reactors Development Laboratory
Korea Hydro and Nuclear Power Co., Ltd

Enclosure:
l. Affidavit KAW-14-0008
2. KHNP Responses to Request for Additional Information No. 2-7371 (Proprietary)
3. KHNP Responses to Request for Additional Information No. 2-7371 (Non-Proprietary)

Cc: Mr. Samuel S. Lee

Non-Proprietary

KHNP
KOREA HYDRO & NUCLEAR POWER CO., LTD

ENCLOSURE 3

" KHNP Responses to Request for Additional Information No. 2-7371" (Non-Proprietary)

April 2014

KHNP Response to Request for Additional Information No. 2-7371

Question 1

Please provide the following documents referenced in the topical report (TR) APR1400-Z-M-TR-12003-P, Rev. 0:
a) Data Base of Fluidic Device Performance Verification Experiment, KAERI/THETA-FD2, Rev.1 (2012)
b) Quality Assurance Manual, APR1400 Fluidic Device Verification Experiment (2003)
c) Quality Assurance Procedures, APR1400 Fluidic Device Verification Experiment (2003)
d) FD Performance Repeatability Experimental Procedure, FD-EP-01 (2004)

Response

The above documents are separately attached as PDF files.
Attachment A. FD Database Report-P.pdf
Attachment A. FD Database Report-NP.pdf
Attachment B. FD Quality Assurance Manual-NP.pdf
Attachment C. FD Quality Assurance Procedures-NP.pdf
Attachment D. FD Experimental Procedure-P.pdf
Attachment D. FD Experimental Procedure-NP.pdf

Question 2

TR section 4.2 describes four (4) cases of tests carried out to verify the performance of the VAPER SIT with test conditions summarized in Tables 4.2-1 through 4.2.5.

a) Are the numbers of test cases sufficient to cover the application range of SIT?
b) What are the ranges of the applicability of the SIT-FD test results in terms of SIT pressure, RCS pressure, temperature, dissolved nitrogen, (other parameters?) etc.?

Response

a) The test cases presented in the topical report with the basis of the above parameters are sufficient to cover the SIT-FD application range. In the early phase of APR1400 SIT-FD, the basic design parameters were determined through the tests conducted at a small scale test facility of [ ]TS Then, the full-scale tests were conducted with the purpose of final design confirmation. In conducting the full scale tests, [ ]TS were considered as the major parameters that affected the performance of the SIT-FD.

b) The applicable ranges of the VAPER SIT-FD test results are provided in Table RAI-2

Table RAI-2 Test range and plant operation range

[ ]TS

1) [ ]TS psig is the initial SIT pressure in Case-01-04 Test.
2) [ ]TS psig corresponds to 95% of plant operation pressure of [ ]TS psig.
3) [ ]TS psig is the RCS pressure which corresponds to the pressure difference of [ ]TS psig between SIT nominal pressure ([ ]TS psig) and RCS pressure.
4) As described in the answer to the APR1400-RAI-16, the two-phase flow formed by the air through the empty stand pipe causes higher pressure drop across the FD than the two-phase flow formed by the evolution of dissolved nitrogen when the gas quality is the same. As described in topical report Section 5.2, the maximum nitrogen gas flow rate is

much smaller than the air flow rate during the period of [ ]^{TS} seconds. Therefore, the VAPER test results cover the range of dissolved nitrogen gas up to the saturated dissolution of nitrogen with respect to its effect on the FD K-factor.

Question 3

Figure 4.3-1 shows the water level changes in the SIT and the stand pipe for Case-01 tests. Section 4.3.1 states that the base elevation of the SIT water level is the bottom of the SIT, and the base elevation of the stand pipe water level is [ ]TS mm higher than the top surface of the FD. As a result, the base elevation of the stand pipe water level is [ ]TS mm higher than that of the SIT water level.

a) Does this mean that the SIT water level shown in Figure 4.3-1 must subtract [ ]TS mm in order to have direct comparison with the stand pipe water level (having the same reference base elevation)?
b) What is the reason for not using the same reference base elevation on the same figure?

Response

a) Yes. We can subtract [ ]TS mm from the SIT water level to have the same base elevation with the stand pipe water level. The following two figures show the locations of the pressure tabs for the measurements of SIT and stand pipe water levels.

b) The water levels were measured using differential pressure transmitters. The pressure impulse lines of the transmitters were connected to the bottom of the SIT for the SIT water level, and to the bottom part of the stand pipe for the stand pipe water level. The actual locations to which the pressure impulse lines were connected were used as the base elevation for each water level. There is no special reason for not using the same base elevation.

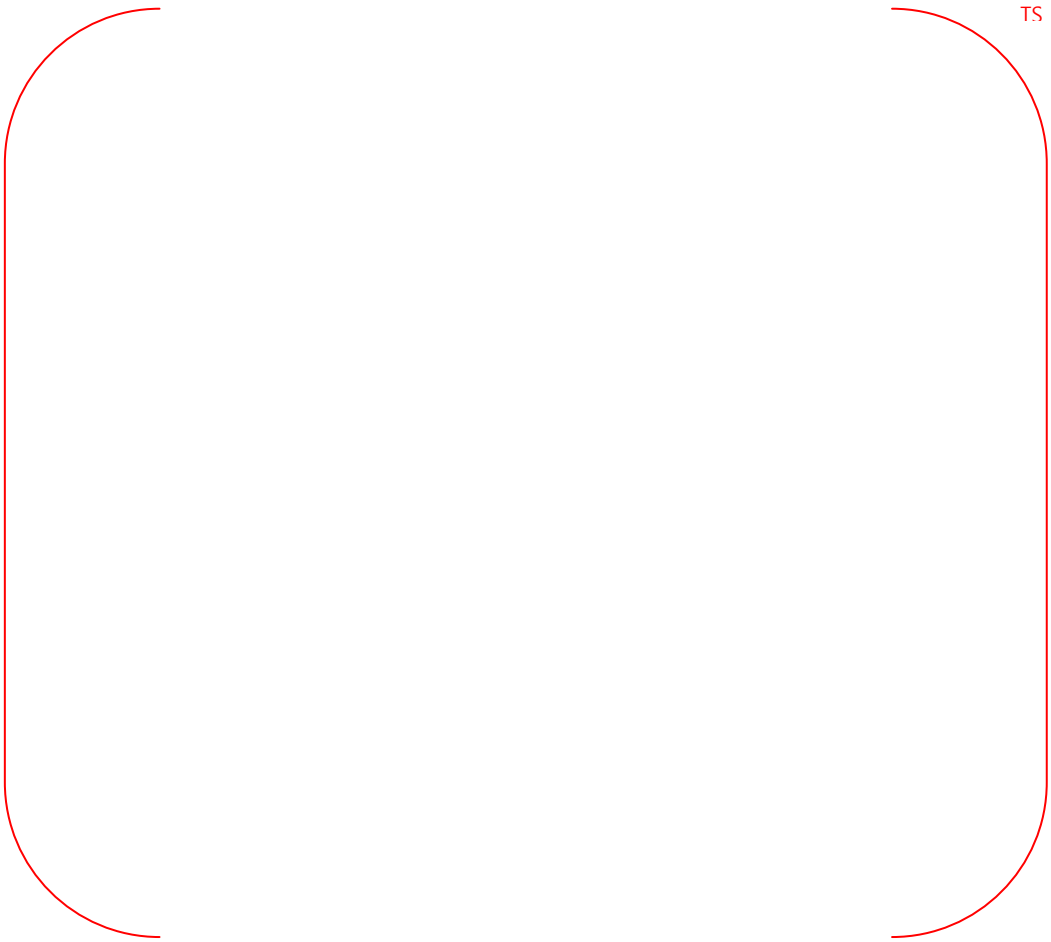

Figure RAI-3 Pressure Tab Locations for SIT and Stand Pipe Water Level Measurements

Question 4

Figure 4.3-2 shows comparison of the water level changes in the SIT and the standpipe for various test cases. Why does Case-02-01 have the stand pipe water level higher than the stand pipe elevation?

Response

The stand pipe used for Case-02 Tests was [ ][TS] *higher than the stand pipe used for other test cases. The pressure tab located in the upper part of the stand pipe was moved [ ]*[TS] *higher in Case-02 Tests, and the SIT water level was also increased by the height increased in the stand pipe to maintain the same SIT water inventory for large flow period.*

Question 5

Section 4.3 describes the FD test results with time-averaged FD K-factors for various test cases summarized in Table 4.3-1. Figure 4.3-6 depicts FD K-factors as a function of time for only the base case of each of the four test cases.
For test cases 02, 03, and 04, please provide the test results for all cases similar to Figure 4.3-5 for test case-01.

Response

The following three figures show the FD K-factor as a function of time for Cases-02, -03, and -04 Tests:

Figure RAI-5-1 Pressure Loss Coefficient (K-factor) of the Fluidic Device (Case-02 Tests)

Figure RAI-5-2 Pressure Loss Coefficient (K-factor) of the Fluidic Device (Case-03 Tests)

Figure RAI-5-3 Pressure Loss Coefficient (K-factor) of the Fluidic Device (Case-04 Tests)

Question 6

Figure 4.3-11 shows the variation of air temperature in the upper region of the VAPER SIT for test Case-01-01.
a) Provide a figure showing the pressure variation on the SIT tank for the same case.
b) Provide plots for the temperature and pressure variation for all other test cases.

Response

a&b) The air temperature in the SIT was measure only for Case-01 Tests. The following two figures show the air temperature and the SIT pressure for Case-01 Tests.

Figure RAI-6-1 Variation of Air Temperature in the Upper Region of the VAPER SIT (Case-01 Tests)

Figure RAI-6-2 Variation of SIT Pressure (Case-01 Tests)

Question 7

Section 4.4 describes uncertainty evaluation. In Equations 4.4-1 and 4.4-2, it appears that a simplification is made such that (∂Y/∂x)=Y/X. Justify this simplification.

Response

The Equations are obtained not by the simplification, but by the partial derivatives of Equations 4.3-1 and 4.3-2 as follows:

$$W_{SI}(t) = \rho_{wtr} A_{SIT} \frac{h_{SIT}(t) - h_{SIT}(t+\Delta t)}{\Delta t}$$

$$\frac{\partial W_{SI}(t)}{\partial \rho_{wtr}} = A_{SIT} \frac{h_{SIT}(t) - h_{SIT}(t+\Delta t)}{\Delta t} = \frac{W_{SI}(t)}{\rho_{wtr}}$$

$$\frac{\partial W_{SI}(t)}{\partial A_{SIT}} = \rho_{wtr} \frac{h_{SIT}(t) - h_{SIT}(t+\Delta t)}{\Delta t} = \frac{W_{SI}(t)}{A_{SIT}}$$

$$\frac{\partial W_{SI}(t)}{\partial \Delta h_{SIT}(t)} = \rho_{wtr} A_{SIT} \frac{1}{\Delta t} = \frac{W_{SI}(t)}{h_{SIT}(t) - h_{SIT}(t+\Delta t)}$$

$$K_{FD} = \Delta P_{FD} \frac{2\rho_{wtr} A_{Pipe}^2}{W_{SI}^2}$$

$$\frac{\partial K_{FD}}{\partial \Delta P_{FD}} = \frac{2\rho_{wtr} A_{Pipe}^2}{W_{SI}^2} = \frac{K_{FD}}{\Delta P_{FD}}$$

$$\frac{\partial K_{FD}}{\partial \rho_{wtr}} = \Delta P_{FD} \frac{2A_{Pipe}^2}{W_{SI}^2} = \frac{K_{FD}}{\rho_{wtr}}$$

$$\frac{\partial K_{FD}}{\partial A_{Pipe}} = \Delta P_{FD} \frac{2\rho_{wtr} \cdot 2A_{Pipe}}{W_{SI}^2} = 2\frac{K_{FD}}{A_{Pipe}}$$

$$\frac{\partial K_{FD}}{\partial W_{SI}} = \Delta P_{FD} 2\rho_{wtr} A_{Pipe}^2 \frac{(-2)}{W_{SI}^3} = -2\frac{K_{FD}}{W_{SI}}$$

$$\left(\frac{\partial K_{FD}}{\partial W_{SI}}\right)^2 = \left(-2\frac{K_{FD}}{W_{SI}}\right)^2 = \left(2\frac{K_{FD}}{W_{SI}}\right)^2$$

Question 8

Section 4.4 provides an uncertainty evaluation, including the effects on the SIT water injection flow rate and FD K-factor of water density, SIT cross-sectional area, and the SIT water level changes within a time interval.

a) Why are uncertainties of other elements, such as the facing angle between the supply nozzle and control nozzle, and DP across the FD measurement (on K-factor calculation) not considered?

b) What are the bases of the uncertainty value assigned to each element, and the sensitivity of each element on the injection flow rate and K-factor?

Response

a) In the early phase of APR1400 SIT-FD, the facing angle was determined through the tests conducted at a small scale test facility of [ ]^{TS}. The full-scale VAPER SIT-FD was manufactured based on that facing angle. The effect of facing angle would be insignificant because the manufacturing tolerance of the facing angle is [ ]^{TS}, thus the uncertainty of the facing angle was not considered.

The uncertainty of the DP measurement across the FD is considered in the first term of RHS in topical report Eq. 4.4-2. As described in topical report Section 4.4, the elemental systematic uncertainty of the DP measurement is [ ]^{TS}.

b) The uncertainty of the water density was determined to cover the density difference between the lowest density at [ ]^{TS} and the highest density at [ ]^{TS}. The above densities cover the whole range of the density in all test cases.
The uncertainty of the SIT cross-sectional area was determined based on the dimensional inspection report provided by the manufacturer of VAPER SIT.
The uncertainties of the SIT level change, DP across the FD was determined based on the on-site calibration results.
The uncertainty of the piping cross-sectional area was set to have the same uncertainty with the SIT cross-sectional area because the dimensional inspection report was not provided.
The references [2] and [3] in the topical report define the sensitivity of the each elemental uncertainty as the partial derivative terms in Equations 4.4-1 and 4.4-2, such as $\frac{\partial K_{FD}}{\partial \Delta P_{FD}}$, $\frac{\partial K_{FD}}{\partial \rho_{wtr}}$, $\frac{\partial K_{FD}}{\partial A_{Pipe}}$, $\frac{\partial K_{FD}}{\partial W_{SI}}$.

Question 9

Section 4.4 determines the total uncertainty of FD K-factors as shown in Figure 4.4-3, and the average total uncertainty of [ ]TS for the large and small flow rate periods, respectively.

a) How are these total uncertainty values combined with the K-factors in Table 4.3-1?
b) In the safety analyses, what are the values of the FD K-factors used for the large and small flow periods, respectively?

Response

a) The uncertainty is not included in the FD K-factors in topical report Table 4.3-1. The systematic uncertainty of the FD K-factor is calculated by the uncertainty propagation equation of Eq. 4.4-2 in topical report. The random uncertainty is calculated by multiplying a coverage factor (t_{95}) to the standard deviation for thirteen FD K-factors presented in Table 4.3-1. The value of [ ]TS was used for the coverage factor, which corresponds to the degree of freedom of twelve (number of K-factors minus one) and 95% confidence level.
As described in topical report Section 4.6, the final FD K-factor of the VAPER tests is obtained by combining the mean value of the thirteen FD K-factors in Table 4.3-1 and the total uncertainty. In case of the large flow injection period, the mean value is [ ]TS and the total uncertainty is [ ]TS. As a result, the final large flow FD K-factor of the VAPER tests has the range of [ ]TS. In case of the small flow injection period, the mean value is [ ]TS and the total uncertainty is [ ]TS. As a result, the final large flow FD K-factor of the VAPER tests has the range of [ ]TS.

b) The safety injection tanks with fluidic device (SIT-FD) are mainly activated during a Large-Break Loss-of-Coolant Accident (LBLOCA).
The CAREM, the realistic evaluation methodology for LBLOCA of the APR1400, uses design requirement values of the FD K-factor for large and small flow injection periods. As described in Section 2.3 of the TR fluidic device design for the APR1400, the design requirement ranges of the total pressure loss coefficient (K-factor) of the FD and safety injection(SI) line form the SIT-FD nozzle to the direct vessel injection (DVI) nozzle are;

[ ]TS

Among the design requirement ranges of K-factor above, the CAREM determines the most conservative K-factors(total pressure loss coefficient of the FD and safety injection(SI) line form the SIT-FD nozzle to the direct vessel injection (DVI) nozzle) based on the sensitivity study. The determined K-factors (total pressure loss coefficient of the FD and SI line form the SIT-FD nozzle to the DVI nozzle) for large and small flow injection periods are;

[ ] TS

The detailed results of the K-factor sensitivity study and modeling of the SIT-FD are described in Appendix H of the TR CAREM.
For small break LOCA (SBLOCA), large flow is injected from SIT-FD during relatively larger breaks and the transient ends before small flow injection phase begins. The FD K-factor of [ ] TS is used for large flow injection phase, based on VAPER test results.

Question 10

Figure 4.3-1 and 4.3-2 show the flow rate turning point (around 30 seconds) when the SIT water level (after subtracting [ ]TS) is close to the stand pipe level.

a) In all tests do the flow rate turning points (switching from large to small flow rate) occur when the SIT water level decreases to the stand pipe elevation?
b) What are the variations of the SIT water level from the stand pipe elevation observed in these test?
c) In the LOCA safety analyses, what is the criterion used to determine the flow rate turning or switchover from the large-flow injection phase to the small-flow injection phases so that the corresponding K-factors can be used?
d) How is the variation or uncertainty of the SIT water level for flow rate switching accounted for in the safety analyses?

Response

a&b) Table RAI-10 shows the Flow Rate Turning Time (Column [A]) and the difference between SIT water level and top elevation of stand pipe height at the flow rate turning time (Column [E]). The flow rate turning time corresponds to the time when the stand pipe water level starts to decrease abruptly.
Column [B] is the SIT water level at the flow rate turning time. Column [C] is the length (or height) of stand pipe. ΔH in Column [D] is the elevation difference from the reference elevation of SIT water level (SIT bottom) to the elevation at the bottom of the stand pipe. ΔH is [ ]TS.
The SIT water level at the flow rate turning time is, on average, [ ]TS higher than the top of the stand pipe. The standard deviation for the difference (Column [E]) is [ ]TS.

c)

[ ]TS

The results of SIT-FD model assessment against VAPER tests show that the SIT-FD model described above reasonably predicts flow rate turning time from large flow injection phase to small flow injection phase. The details of SIT-FD model assessments are described in Appendix H of TR CAREM.

d)

TS

Table RAI-10 SIT Water Level at Flow Rate Turning Time

TS

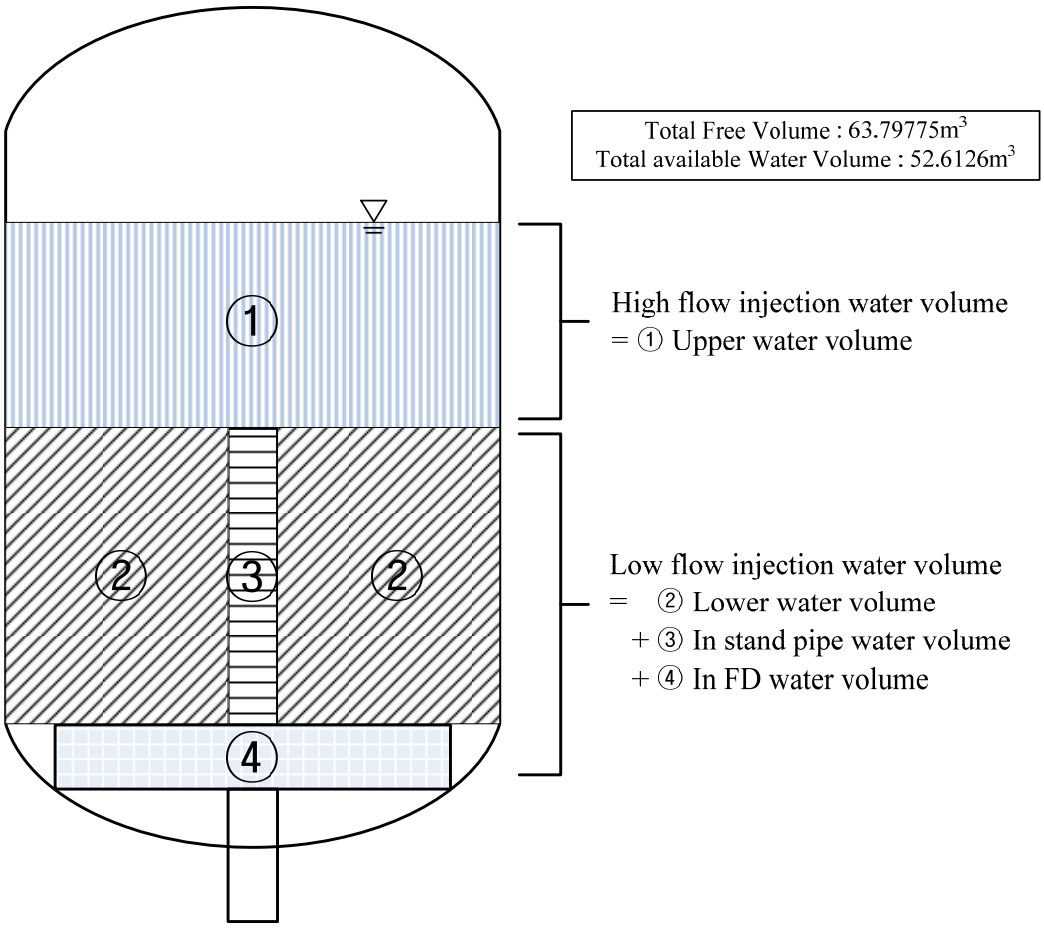

Figure RAI-10 A schematic diagram of the SIT-FD

Question 11

Section 4.1.3 states that the pressure of the stock tank is kept to be an atmospheric pressure condition during the experiment. During a LOCA, the RCS pressure will fluctuate during the transient.
What is the effect of dynamic RCS pressure fluctuations on the K-factors? Is there additional uncertainty due to this dynamic pressure fluctuation effect and how is the uncertainty, if any, accounted for?

Response

As can be seen from the Case-01-04 test result, the FD K-factor was not affected when the pressure difference between SIT and RCS was reduced to about [ ]^{TS}. Rapid pressure transient of RCS occurs in large flow period, and a swirling flow in the fluidic device does not appear during that period. Therefore, the effect of system pressure on the FD K-factor has similarity to the effect of system pressure on the discharge coefficient of venture device, which is insignificant as generally accepted.
The rate of change in the pressure difference between SIT and RCS might affect the FD K-factor. Figure RAI-11 shows the typical pressure difference change calculated by RELAP 5/MOD3 for APR1400 LBLOCA, and the pressure difference changes obtained from the VAPER tests (Case-01-04 and Case-01-04). The effect of the pressure difference change of APR1400 is covered by the VAPER tests.
Therefore, we determined that the K-factor would not be affected by the RCS dynamic pressure fluctuation, and the uncertainty due to this pressure fluctuation was not considered.

Figure RAI-11 Changes in the pressure difference between SIT and RCS

Question 12

Test Case-01-04 has the initial SIT tank pressure of [ ]TS, which is about [ ]TS of the initial SIT pressure of [ ]TS psig for all other test cases. Section 4.3.3 states that as indicated in Table 4.3-1, Case-01-04 test showed that the pressure loss coefficient of the FD was not dependent on pressure difference between the SIT and the RCS. However, Table 4.3-1 shows that the time-averaged FD K-factor of [ ]TS for the large-flow phase for Case 01-04 is lower than all other cases with K factor of [ ]TS.
Please clarify the statement that the FD K-factor was not dependent on the SIT-RCS pressure difference.

Response

In order to examine the effect of the pressure difference between SIT and RCS on the FD K-factor, we should compare the test results which have the same test conditions except the pressure difference between SIT and RCS. That is, the FD K-factor of Case-01-04 should be compared with the FD K-factors of Case-01-01, Case-01-02, and Case-01-03.
The average difference between the FD K-factor of Case-01-04 and the other three FD K-factors is [ ]TS. The standard deviation of the three FD K-factors of Case-01-01, Case-01-02, and Case-01-03 is [ ]TS, and the 't' value of t-distribution with 95% confidence level is [ ]TS. As a result, the random uncertainty for the three FD K-factors is [ ]TS.
The average difference of [ ]TS between Case-01-04 and the other three test cases is less than half of the random uncertainty of [ ]TS, thus it falls within the uncertainty range with sufficient margin. Therefore, we can conclude that the FD K-factor is not dependent on the SIT-RCS pressure difference.

Question 13

Figure A-5 of Appendix A of the TR, titled "Drawing of the SIT and FD of the VAPER Facility," shows the drawing of the discharge pipe connected to the exit nozzle, with the inside diameter of the discharge pipe of [ ]TS mm. This appears to be contrary to the statement in Sections 4.1.3 and 5.1 that the inner diameter of the discharge pipe line of the VAPER test facility is [ ]TS mm, which is also different from the diameter of the SI discharge line ([ ])TS of the APR1400.

a) Do figures in Appendix A represent the dimensions for the VAPER test facility or the APR1400 design?
b) Are the drawings of the exit nozzle drawing and discharge pipe in Figures A-4 and A-5 representing VAPER facility or APR1400?
c) What are the exit nozzle dimensions for the VAPER facility and APR1400?

Response

a) Figures A-1 to A-4 in Appendix A of the TR represent the dimensions for the VAPER test facility. But, figures A-5 represents neither the VAPER test facility nor the APR1400 design. Figure A-5 was inadvertently included in the report. The TR will be revised replacing this figure with the correct figure, which represents the dimension for the VAPER test facility.

b) Figures A-5 represents neither the VAPER test facility nor the APR1400 design. Figure A-4, which is a correct figure, represents the VAPER test facility. Figure A-5 was inadvertently included in the report. The TR will be revised replacing this figure with the correct figure, which represents the dimension for the VAPER test facility.

c) Figures RAI-13-1 shows the discharge tube of the VAPER SIT-FD. Figure RAI-13-2 and RAI-13-3 show the exit nozzle and discharge tube of the APR1400 SIT-FD. Major dimensions of each of the exit nozzle and discharge tube are presented in Table RAI-13.

Table RAI-13 Dimensions of exit nozzles and discharge tubes of VAPER SIT-FD and APR1400 SIT-FD

TS

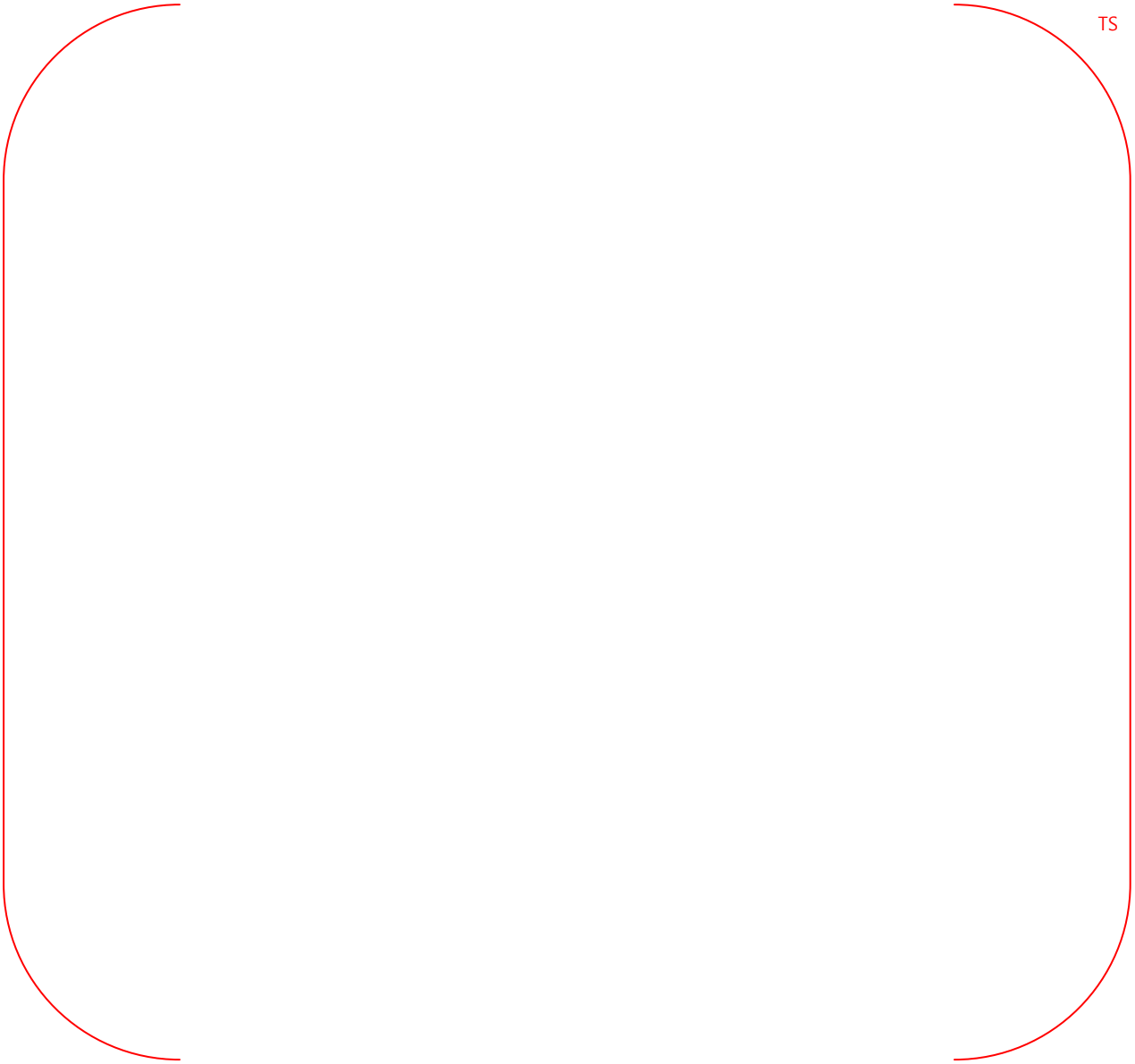

Figure RAI-13-1 Drawing of Discharge Tube of VAPER SIT-FD

Figure RAI-13-2 Drawing of Exit Nozzle of APR1400 SIT-FD

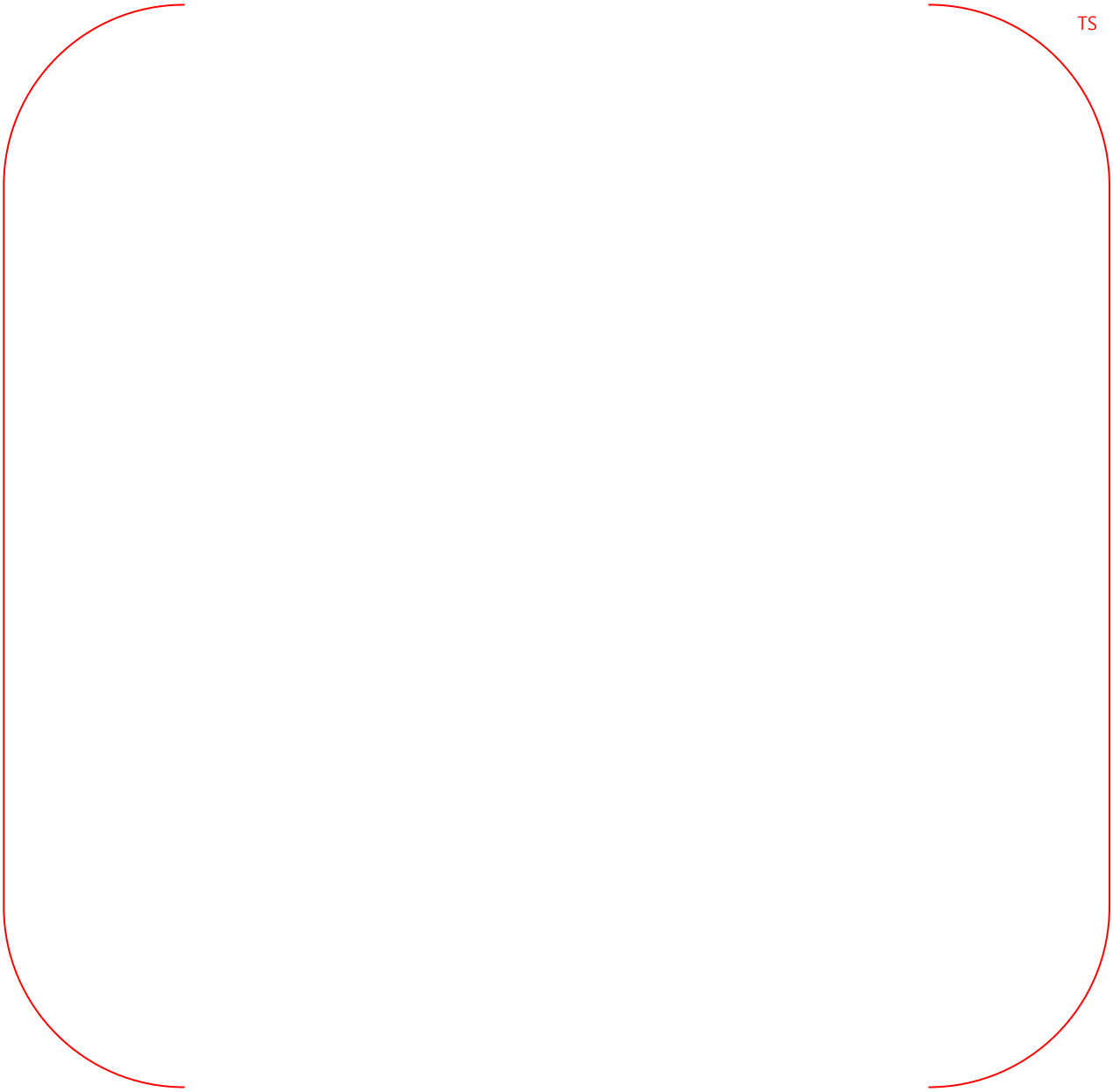

Figure RAI-13-3 Drawing of Discharge Tube of APR1400 SIT-FD

Question 14

Section 4.3.4 provides a calculation of air discharge from the SIT, and shows the inception of air discharge at around [ ]TS for Test Case-01. It also provides the average values of the FD K-factor for the periods of [ ]TS seconds, [ ]TS seconds, and [ ]TS seconds, from the evaluation of the case 01-01 test at the small flow condition, which shows a variation of about [ ]TS. It then concludes that the difference among the FD K-factor averaged over different time periods would be primarily due to random unsteadiness of the swirling flow inside the vortex chamber of the FD, and the FD K-factor was not sensitive to the amount of air discharge flow rate for the period of [ ]TS seconds. Please explain how KHNP arrived at this conclusion?

Response

Short term random fluctuations are expected due to very short fluctuations in turbulent flow and instrument noise. A short term fluctuation of the SIT water level measurement results in an amplified short term time variation of the FD K-factor.

The FD K-factor is inversely proportional to the square of the SI water injection flow rate (Eq. 4.3-2 in TR), and the SI water injection flow rate is proportional to the time derivative of the SIT water level (Eq. 4.3-1 in TR). As a result, the FD K-factor is inversely proportional to the square of the time derivative of the SIT water level, and a subtle change in the SIT water measurement is amplified in the FD K-factor calculation, thus causing the time variation of the FD K-factor.

The random error in the SIT water level measurement randomly affects the FD K-factor calculation throughout the whole period of the SI water injection.

Figure RAI-14 shows the small flow FD K-factors of Case-01 tests (Case-01-01, 01-02, and 01-03), which are averaged for ten seconds. The time averaged FD K-factors show a periodicity, but the periodicity has still random characteristics (i.e., the times of the peaks and valleys are different among the tests). As a result, the time variation of the FD K-factor is not wholly related with the short term random fluctuation, but also related with a long term fluctuation. We presumed that it would be the unsteadiness of the swirling flow inside the vortex chamber.

Comparing the K-factors for a period of [ ]TS seconds and [ ]TS seconds during which the air discharges throughout an empty stand pipe, there is not a noticeable change in the FD K-factor. As a result, we can conclude that FD K-factor is not sensitive to the amount of air discharge flow rate for the period of [ ]TS seconds.

TS

Figure RAI-14 Averaged FD K-factors of Case-01 tests

Question 15

There is no discussion of whether cavitation occurs in the vortex chamber or the exit nozzle.

a) Has cavitation been observed in the vortex chamber or exit nozzle during large flow and small flow injection phases in any of the tests? If cavitation was not observed in the tests, does it mean cavitation did not occur, or it might have occurred but was not detected because no means was provided to detect cavitation?
b) Has a calculation been made to determine whether cavitation could occur in the vortex chamber or the exit nozzle? What is the lowest pressure calculated or measured in the vortex chamber and at the throat of exit nozzle? Are the pressures in these areas lower than the vapor pressure so that cavitation would occur?
c) What would be the effects of cavitation, if it occurs, on the SIT flow rates and FD K-factors for both large and small flow periods.

Response

a) Cavitation was not detected because no means was provided to detect cavitation in all the cases of VAPER tests.

b&c) KHNP will provide CFD analysis results which include a cavitation effect on the SIT-FD performance (FD K-factors) and a series of sensitivity analysis to support for a validation of CFD methodology.

Question 16

Section 5.2 discusses the effect of dissolved nitrogen gas on the FD K-factor. It concludes that the maximum mass and volumetric flow rate of nitrogen gas are much smaller than the air discharge flow rate during the period of [ ]^{TS} seconds, and as a result, the evolution of dissolved nitrogen gas does not materially affect the FD K-factor.

Since the air discharge is the discharge of covered air when the standpipe is emptying, which is different from the evolution of the dissolve nitrogen in the SIT water, how can it be used as a comparison for the dissolved nitrogen coming out of SIT water?

Response

In case that the evolution of dissolved nitrogen occurs, it is mixed with SI water and two-phase flow is formed. For the same mass flow rate, we expect that the pressure drop in two-phase flow is higher than that in single-phase flow. In case that a gas quality is low, the pressure drop increases with an increase in the gas quality. In case that a flow path is the same, the pressure drop increases with an increase in the migration length of the two-phase flow in the flow path.

The throat of the FD exit is the place where the pressure reaches its minimum. Therefore, the region near the FD exit is the most vulnerable place to the gaseous cavitation due to the evolution of dissolved nitrogen. On the other hand, in case that the air flows into the FD vortex chamber, two-phase flow starts to be formed from the exits of supply nozzle and control nozzle. That is the two-phase flow migrates whole through the vortex chamber and discharge tube. As a result, the two-phase flow formed by the air through an empty stand pipe has longer migration length. Thus, the air flow causes higher pressure drop than the evolution of dissolved nitrogen when the gas quality is the same for both cases. As described in topical report Section 5.2, the maximum nitrogen gas flow rate is much smaller than the air discharge flow rate during the period of [ ]^{TS} seconds. Therefore, we expect that the evolution of dissolved nitrogen gas does not materially affect the FD K-factor.

Question 17

Each supply nozzle has a facing angle of [ ]TS with a neighboring control nozzle in the vortex chamber in order to minimize the swirling flow effect.

a) How is this facing angle of [ ]TS determined to be appropriate?
b) What is the manufacturing uncertainty of this facing angle?
c) What is the effect of the facing angle uncertainty on the K-factor of large flow period?

Response

a) In the early phase of APR1400 SIT-FD, the basic design parameters were determined through the tests using a small scale test facility of AEA Technology in U.K. Tests were conducted for two FDs which have the facing angles of [ ]TS. Based on the test results, the facing angle of [ ]TS was selected as a basic design parameter.

b) The manufacturing tolerance or uncertainty of the facing angle is [ ]TS.

c) KHNP will provide CFD analysis results which include a facing angle effect (under a manufacturing tolerance band) on the SIT-FD performance (FD K-factors) and a series of sensitivity analysis to support for a validation of CFD methodology.

Question 18

Since the FD verification test results are applicable to the specific FD design configuration, what process will be used to assure that no changes are made to the APR1400 SIT/FD design configuration?

Response

SIT-FD (FD) design is followed by configuration control process as follows. KAERI produced the Full Scale Test results as stated in the topical report and performed an internal QA process during design confirmation. The final FD design in U.S. will be provided to KHNP from KAERI, and then KHNP will provides the final FD design to the manufacturer, Doosan Heavy Industry (DHI), after KHNP's internal QA process. DHI will perform its internal QA process at manufacture stage. Configuration Control for the FD design will be properly maintained since each organization performs own internal QA process. KHNP is responsible for all the processes
The main parameters of the SIT-FD such as SIT water volume, K-factor for large and small flow period will be described in ITAAC. Figure RAI-18 is shows a draft ITAAC for the FD design.

Table RAI-18 A draft ITAAC for the FD design

TS

Page intentionally left blank

SECTION D

Page intentionally left blank

Non-Proprietary

KHNP
KOREA HYDRO & NUCLEAR POWER CO., LTD
70-1312-gil, Yuseong-daero, Yuseong-gu, Daejeon, 305-343, KOREA
Tel: +82-42-870-5740 / Fax: +82-42-870-5779
http://www.khnp.co.kr

June 11, 2014
Document Control Desk
U.S. Nuclear Regulatory Commission
Washington, DC 20555-0001

Attention: Mr. Jeffrey Ciocco
Division of New Reactor Licensing

Project No.0782
MKD/NW-14-0017L

Subject: KHNP Response to RAI 2-7371 on Question 15-b, 15-c, and 17-c

Reference: 1) NRC Request for Additional Information 2-7371, dated March 11, 2014
2) KHNP Topical Report: Fluidic Device Design for the APR1400, Revision 0, December 2012 (APR1400-Z-M-TR-12003)
3) KHNP Letter to NRC: MKD/NW-14-0008L, "Submittal of KHNP Responses to Request for Additional Information 2-7371", dated April 11, 2014

KHNP is hereby submitting responses to the Request for Additional Information (RAI) 2-7371, dated March 11, 2014. This RAI response addresses question 15-b, 15-c, and 17-c of the RAI 2-7371.In addition, one technical report, "CFD Analysis of Fluidic Device" is submitted as well.

Enclosure 1 contains one copy of the associated affidavit. Enclosure 2 provides "KHNP Response to Request for Additional Information No 2-7371" (Proprietary), and Enclosure 3 provides "KHNP Response to Request for Additional Information No 2-7371" (Non-proprietary). Finally, Enclosure 4 provides "CFD Analysis of Fluidic Device" (proprietary), and Enclosure 5 provides "CFD Analysis of Fluidic Device" (Non-proprietary).

If additional information or clarification is required, please contact Yunho Kim, Director of KHNP Washington DC Center at yunhokim@khnp.co.kr or 703-388-0592.

Sincerely,

M. K. Kim

Myung-Ki Kim
Project Manager
Advanced Reactors Development Laboratory
Korea Hydro and Nuclear Power Co., Ltd

KHNP
KOREA HYDRO & NUCLEAR POWER CO., LTD

Enclosure:
l. Affidavit KAW-14-0017
2. KHNP Responses to Request for Additional Information No. 2-7371 (Proprietary)
3. KHNP Responses to Request for Additional Information No. 2-7371 (Non-Proprietary)
4. Technical Report, “CFD Analysis of Fluidic Device” (proprietary) (APR1400-K-A-NR-14005-P)
5. Technical Report, “CFD Analysis of Fluidic Device” (Non-proprietary) (APR1400-K-A-NR-14005-NP)

Non-Proprietary

KHNP
KOREA HYDRO & NUCLEAR POWER CO., LTD

ENCLOSURE 3

" KHNP Responses to Request for Additional Information No. 2-7371"
(Non-Proprietary)

June 2014

RESPONSES TO REQUEST FOR ADDITIONAL INFORMATION 2-7371

Date of RAI Issued: 03/11/2014
Response Date: 06/11/2014

Question 15

There is no discussion of whether cavitation occurs in the vortex chamber or the exit nozzle.

b) Has a calculation been made to determine whether cavitation could occur in the vortex chamber or the exit nozzle? What is the lowest pressure calculated or measured in the vortex chamber and at the throat of exit nozzle? Are the pressures in these areas lower than the vapor pressure so that cavitation would occur?
c) What would be the effects of cavitation, if it occurs, on the SIT flow rates and FD K-factors for both large and small flow periods.

Response

b) Based on the CFD analysis, the vaporous cavitation can occur in the center of the exit nozzle and the discharge tube in both large and small flow mode. In the Test Case-01-01, the temperature of water is [ ]TS and its saturation pressure of vapor is about [ ]TS. Therefore, the local pressure in the center region of the exit nozzle and the discharge tube is calculated as [ ]TS. More detailed information for the flow structure and the formation of vaporous cavitation are provided in the Technical Report, "CFD Analysis of Fluidic Device".

c) In the full scale experiment, there were no instruments to detect the cavitation.
The CFD analysis is performed to predict cavitation phenomena and its related to the performance of the SIT-FD. First, the boundary conditions of the CFD analysis are fixed using the test data, and then the performance of the SIT-FD, K-factor is predicted using the cavitation model. If the CFD results indicate good similarity for measured K-factor, predicted flow structure and cavitation can be justified.
As above mentioned, the SIT flow rates of the test data are used for the boundary conditions of the CFD analysis thus the SIT flow rates should be same with the test data to satisfy the continuity equation in the governing equations as shown in Figure RAI-15-2.
The CFD evaluated K-factors in some cases are deviated from the uncertainty ranges of the test but all cases are similar with the test data as shown in Figure RAI-15-1 and Figure RAI-15-2.
The CFD results show the occurrence of vaporous caviation in the center of the exit nozzle and the discharge tube in both large and small flow mode. However, there was no effect of the pressure loss in the FD by a flow blockage due to the vaporous cavitation.

Table RAI-15 CFD analysis results for large flow and small flow mode

TS

TS

Figure 15-1 Comparison between the test results and CFD evaluated results for K-factor

TS

Figure 15-2 Comparison between the test results and CFD evaluated results for mass flow rate

TS

Figure 15-3 Comparison between the test results and CFD evaluated results for differential pressure of the FD

Question 17

Each supply nozzle has a facing angle of [ ]TS with a neighboring control nozzle in the vortex chamber in order to minimize the swirling flow effect.

c) What is the effect of the facing angle uncertainty on the K-factor of large flow period?

Response

c) Table RAI-17-1 shows the results for facing angle sensitivity analysis using the CFD code. In large flow mode, the maximum difference of CFD evaluated K-factor between the distorted design and the normal design is [ ]TS in L1 case. In small flow mode, the maximum difference of K-factor between the distorted design and the normal design is [ ]TS. As described in the TR of the SIT-FD, The total uncertainty of K-factor is [ ]TS in the large flow mode, and is [ ]TS in the small flow mode. The CFD evaluated K-factors in small flow mode are within the uncertainty ranges of the test results but the K-factors in large flow mode are deviated from the uncertainty ranges.

Meanwhile, the design requirement ranges of the K-factor from the SIT-FD to DVI nozzle are;

[ ]TS

Since the range of the K-factor of the expected SI line from the SIT-FD nozzle to the DVI nozzle is [ ]TS hence the design requirement ranges of the FD K-factor are;

[ ]TS

Using these ranges of K-factor above, LBLOCA calculation is performed and the results have enough margins to meet the acceptance criteria.

In conclusion, the facing angle effect originated from the manufacturing tolerance has not a significant effect on the performance of the SIT-FD.

Table RAI-17-1 Analysis results for the facing angle sensitivity analysis

TS

Page intentionally left blank

SECTION E

Page intentionally left blank

Non-Proprietary

KHNP
KOREA HYDRO & NUCLEAR POWER CO., LTD
70-1312-gil, Yuseong-daero, Yuseong-gu, Daejeon, 305-343, KOREA
Tel: +82-42-870-5740 / Fax: +82-42-870-5779
http://www.khnp.co.kr

April 23, 2015
Document Control Desk
U.S. Nuclear Regulatory Commission
Washington, DC 20555-0001

Attention: Mr. Jeff Ciocco
Division of New Reactor Licensing

Docket No. 52-046
MKD/NW-15-0009L

Subject: Revised Response to RAI 2-7371

Reference: NRC Request for Additional Information 2-7371, dated March 11, 2014

KHNP is hereby submitting revised response to the Request for Additional Information (RAI) 2-7371, dated March 11, 2014 as discussed with the NRC staff during the teleconference held on March 30, 2015. This RAI response addresses questions 16 of the RAI 2-7371.

Enclosure 1 contains one copy of the associated affidavit. Enclosure 2 provides Revised Response to RAI 2-7371 on Topical Report "Fluidic Device Design for the APR1400" APR1400-Z-M-TR-12003-P, Rev.0 (Proprietary), and Enclosure 3 provides Revised Response to RAI 2-7371 on Topical Report "Fluidic Device Design for the APR1400" APR1400-Z-M-TR-12003-NP, Rev.0 (Non-proprietary).

If additional information or clarification is required, please contact Yunho Kim, director of KHNP Washington DC center at yunho.kim@khnp.co.kr or 703-388-0592.

Sincerely,

M. K. Kim

Myung-Ki Kim
Project Manager
Advanced Reactors Development Laboratory
Korea Hydro and Nuclear Power Co., Ltd

Enclosures:
l. Affidavit KAW-15-0009
2. Revised Response to RAI 2-7371 on Topical Report "Fluidic Device Design for the APR1400" APR1400-Z-M-TR-12003-P, Rev.0 (Proprietary)
3. Revised Response to RAI 2-7371 on Topical Report "Fluidic Device Design for the APR1400"APR1400-Z-M-TR-12003-NP, Rev.0 (Non-proprietary)

Enclosure 3

Docket No. 52-046

Revised Response to RAI 2-7371 on Topical Report
"Fluidic Device Design for the APR1400"
APR1400-Z-M-TR-12003-NP, Rev. 0

April 2015

Non-proprietary Version

RESPONSE TO REQUEST FOR ADDITIONAL INFORMATION

APR1400 Design Certification

Korea Electric Power Corporation / Korea Hydro & Nuclear Power Co., LTD

Docket No. 52-046

RAI No.:	**2-7371 Question 16**
SRP Section:	**N/A**
Application Section:	**Fluidic Device Design for the APR1400 (APR1400-Z-M-TR-12003-P, Rev. 0)**
Date of RAI Issued:	**03/11/2014**
Response Date:	**04/23/2015**

Question 16

Section 5.2 discusses the effect of dissolved nitrogen gas on the FD K-factor. It concludes that the maximum mass and volumetric flow rate of nitrogen gas are much smaller than the air discharge flow rate during the period of [ ]^{TS} seconds, and as a result, the evolution of dissolved nitrogen gas does not materially affect the FD K-factor.

Since the air discharge is the discharge of covered air when the standpipe is emptying, which is different from the evolution of the dissolve nitrogen in the SIT water, how can it be used as a comparison for the dissolved nitrogen coming out of SIT water?

Response

In case that the evolution of dissolved nitrogen occurs, it is mixed with SI water and two-phase flow is formed. For the same mass flow rate, we expect that the pressure drop in two-phase flow is higher than that in single-phase flow. In case that a gas quality is low, the pressure drop increases with an increase in the gas quality. In case that a flow path is the same, the pressure drop increases with an increase in the migration length of the two-phase flow in the flow path.

The throat of the FD exit is the place where the pressure reaches its minimum. Therefore, the region near the FD exit is the most vulnerable place to the gaseous cavitation due to the evolution of dissolved nitrogen. On the other hand, in case that the air flows into the FD vortex chamber, two-phase flow starts to be formed from the exits of supply nozzle and control nozzle. That is the two-phase flow migrates whole through the vortex chamber and discharge tube. As a result, the two-phase flow formed by the air through an empty stand pipe has longer migration length. Thus, the air flow causes higher pressure drop than the evolution of dissolved nitrogen when the gas quality is the same for both cases. As described in topical report Section 5.2, the maximum nitrogen gas flow rate is much smaller than the air discharge flow rate during the period of [ ]^{TS} seconds. Therefore, we expect that the evolution of dissolved nitrogen gas

does not materially affect the FD K-factor.

In the clarification phone call talking, the NRC figured out errors in Table 5.2-1 and 5.2-2 of the topical report.
The nitrogen solubility numbers in the far right column of Table 5.2-1 are obviously typos. However, we confirmed that the curve fitted equations of 5.2-1 and 5.2-2 were correct, and the nitrogen gas release rate (Fig. 5.2-1 and 5.2-2) were correctly calculated from the equations of 5.2-1~5.2-4. The topical report will be revised replacing Table 5.2-1 and 5.2-2 with corrected tables as shown in attachment.

Impact on DCD

There is no impact on the DCD.

Impact on Technical/Topical/Environmental Report

Topical Report APR1400-Z-M-TR-12003-NP will be revised as indicated on the attached markups.

Attachment to Revised Response to RAI 1091-7447 (1/2)

Table 5.2-1 N_2 Solubility (kg/kg_{water}) in Pure Water at 0 °C (32 °F)

P [MPa(a) (psia)]	Solubility (kg/kg_{water})	
	Sun et al. [7]	Eq. 5.2-1
0.1 (14.5)		
0.5 (72.5)		
1.0 (145)		
2.5 (363)		
5.0 (725)		

Table 5.2-2 N_2 Solubility (kg/kg_{water}) in Pure Water at 40 °C (104 °F)

P [MPa(a) (psia)]	Solubility (kg/kg_{water})	
	Sun et al. [7]	Eq. 5.2-2
0.1 (14.5)		
0.5 (72.5)		
1.0 (145)		
2.5 (363)		
5.0 (725)		

Modify to next page

Attachment to Revised Response to RAI 1091-7447 (2/2)

Table 5.2-1 N_2 Solubility (kg/kg_{water}) in Pure Water at 0 °C (32 °F)

P [MPa(a) (psia)]	Solubility (kg/kg_{water})	
	Sun et al. [7]	Eq. 5.2-1
0.1 (14.5)		TS
0.5 (72.5)		
1.0 (145)		
2.5 (363)		
5.0 (725)		

Table 5.2-2 N_2 Solubility (kg/kg_{water}) in Pure Water at 40 °C (104 °F)

P [MPa(a) (psia)]	Solubility (kg/kg_{water})	
	Sun et al. [7]	Eq. 5.2-2
0.1 (14.5)		TS
0.5 (72.5)		
1.0 (145)		
2.5 (363)		
5.0 (725)		

Page intentionally left blank

SECTION F

Page intentionally left blank

Non-Proprietary

KHNP
KOREA HYDRO & NUCLEAR POWER CO., LTD
70-1312-gil, Yuseong-daero, Yuseong-gu, Daejeon, 305-343, KOREA
Tel: +82-42-870-5740 / Fax: +82-42-870-5779
http://www.khnp.co.kr

June 15, 2015
Document Control Desk
U.S. Nuclear Regulatory Commission
Washington, DC 20555-0001

Attention: Mr. Jeff Ciocco
Division of New Reactor Licensing

Docket No. 52-046
MKD/NW-15-0027L

Subject: Revised Response to RAI 2-7371 on Question 13

Reference: 1) NRC Request for Additional Information 2-7371, dated March 11, 2014
2) KHNP Topical Report: Fluidic Device Design for the APR1400, Revision 0, December 2012 (APR1400-Z-M-TR-12003)
3) KHNP Letter to NRC: MKD/NW-14-0008L, "Submittal of KHNP Responses to Request for Additional Information 2-7371", dated April 11, 2014

KHNP is hereby submitting the revised response to RAI 2-7371 dated March 11, 2014. The RAI response addresses question of TR Fluidic Device Design for the APR1400-13.

Enclosure 1 contains a copy of the associated affidavit. Enclosure 2 contains the revised response to RAI 2-7371 on Question 13 (Proprietary), and Enclosure 3 contains the revised response to RAI 2-7371 on Question 13 (Non-Proprietary).

If additional information or clarification is required, please contact Yunho Kim, Director of KHNP Washington DC Center at yunho.kim@khnp.co.kr or 703-388-0592.

Sincerely,

M. K. Kim

Myung-Ki Kim
Project Manager
Advanced Reactors Development Laboratory
Korea Hydro and Nuclear Power Co., Ltd

Enclosures:
1. Affidavit KAW-15-0027
2. Response to RAI 2-7371 on Question 13 (Proprietary)
3. Response to RAI 2-7371 on Question 13 (Non-Proprietary)

Non-Proprietary

KHNP
KOREA HYDRO & NUCLEAR POWER CO., LTD

Enclosure 3

Response to RAI 2-7371 on Question 13

(Non-Proprietary)

June 15, 2015

REVISED RESPONSE TO REQUEST FOR ADDITIONAL INFORMATION

APR1400 Design Certification

Korea Electric Power Corporation / Korea Hydro & Nuclear Power Co., LTD

Docket No. 52-046

RAI No.:	**2-7371 Question 13**
SRP Section:	**N/A**
Application Section:	**Fluidic Device Design for the APR1400 (APR1400-Z-M-TR-12003-P, Rev. 0)**
Date of RAI Issued:	**03/11/2014**

Question 13

Figure A-5 of Appendix A of the TR, titled "Drawing of the SIT and FD of the VAPER Facility," shows the drawing of the discharge pipe connected to the exit nozzle, with the inside diameter of the discharge pipe of [ ]^{TS} mm. This appears to be contrary to the statement in Sections 4.1.3 and 5.1 that the inner diameter of the discharge pipe line of the VAPER test facility is [ ]^{TS} mm, which is also different from the diameter of the SI discharge line ([ ]^{TS}) of the APR1400.

a) Do figures in Appendix A represent the dimensions for the VAPER test facility or the APR1400 design?
b) Are the drawings of the exit nozzle drawing and discharge pipe in Figures A-4 and A-5 representing VAPER facility or APR1400?
c) What are the exit nozzle dimensions for the VAPER facility and APR1400?

Response

a) Figures A-1 to A-4 in Appendix A of the TR represent the dimensions for the VAPER test facility. But, figures A-5 represents neither the VAPER test facility nor the APR1400 design. Figure A-5 was inadvertently included in the report. The TR will be revised replacing this figure with the correct figure, which represents the dimension for the VAPER test facility.

b) Figure A-5 represents neither the VAPER test facility nor the APR1400 design. Figure A-4, which is a correct figure, represents the VAPER test facility. Figure A-5 was inadvertently included in the report. The TR will be revised replacing this figure with the correct figure, which represents the dimension for the VAPER test facility.

c) Figure RAI-13-1 shows the discharge tube of the VAPER SIT-FD. Figure RAI-13-2 and RAI-13-3 show the exit nozzle and discharge tube of the APR1400 SIT-FD. Major dimensions of each of the exit nozzle and discharge tube are presented in Table RAI-13.

Impact on DCD

There is no impact on the DCD.

Impact on PRA

There is no impact on the PRA.

Impact on Technical/Topical/Environmental Report

Topical Report APR1400-Z-M-TR-12003-P will be revised as indicated on the attached markups.

Impact on Technical Specifications

There is no impact on the Technical Specifications.

Table RAI-13 Dimensions of exit nozzles and discharge tubes of VAPER SIT-FD and APR1400 SIT-FD TS

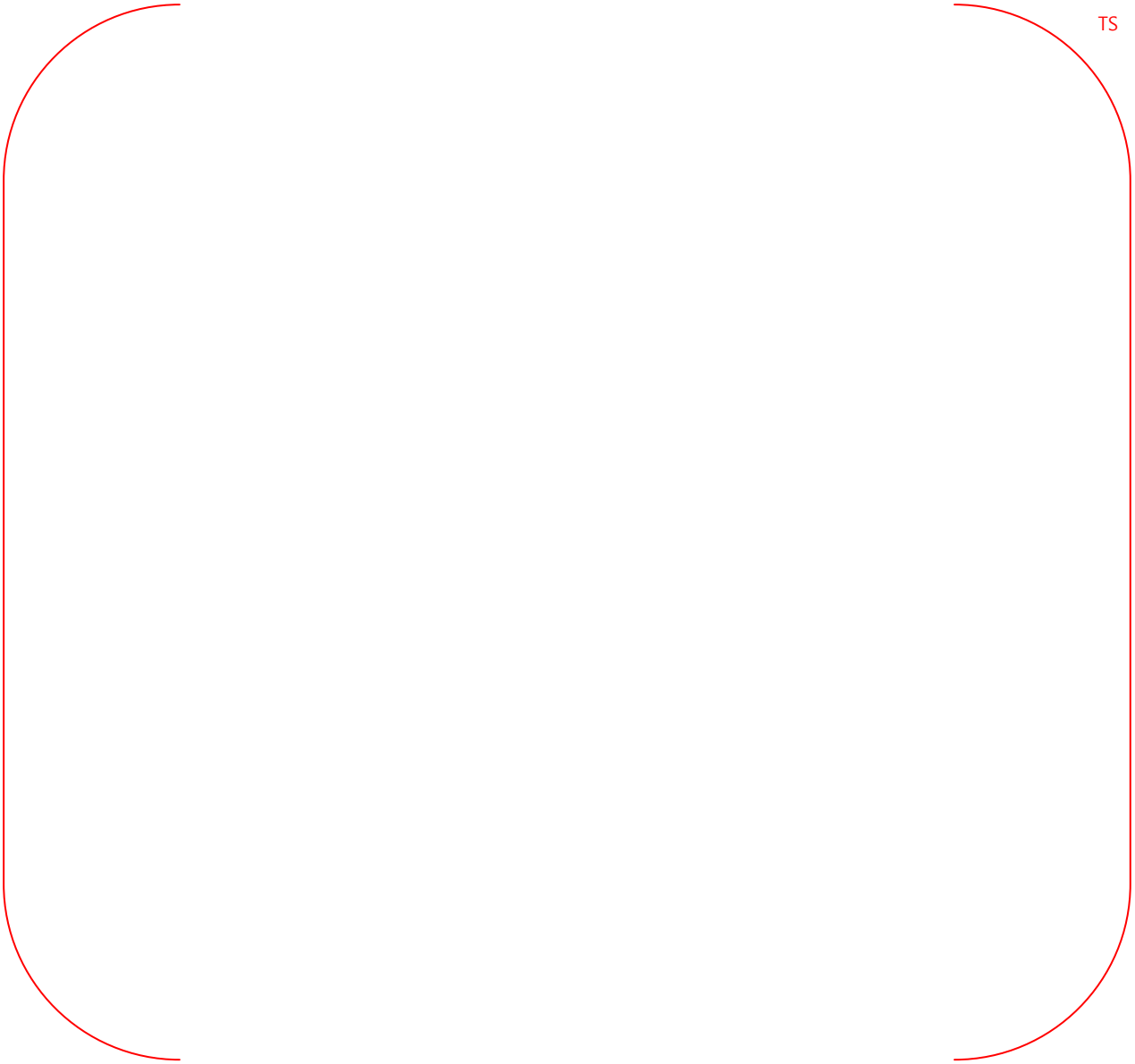

Figure RAI-13-1 Drawing of Discharge Tube of VAPER SIT-FD

Figure RAI-13-2 Drawing of Exit Nozzle of APR1400 SIT-FD

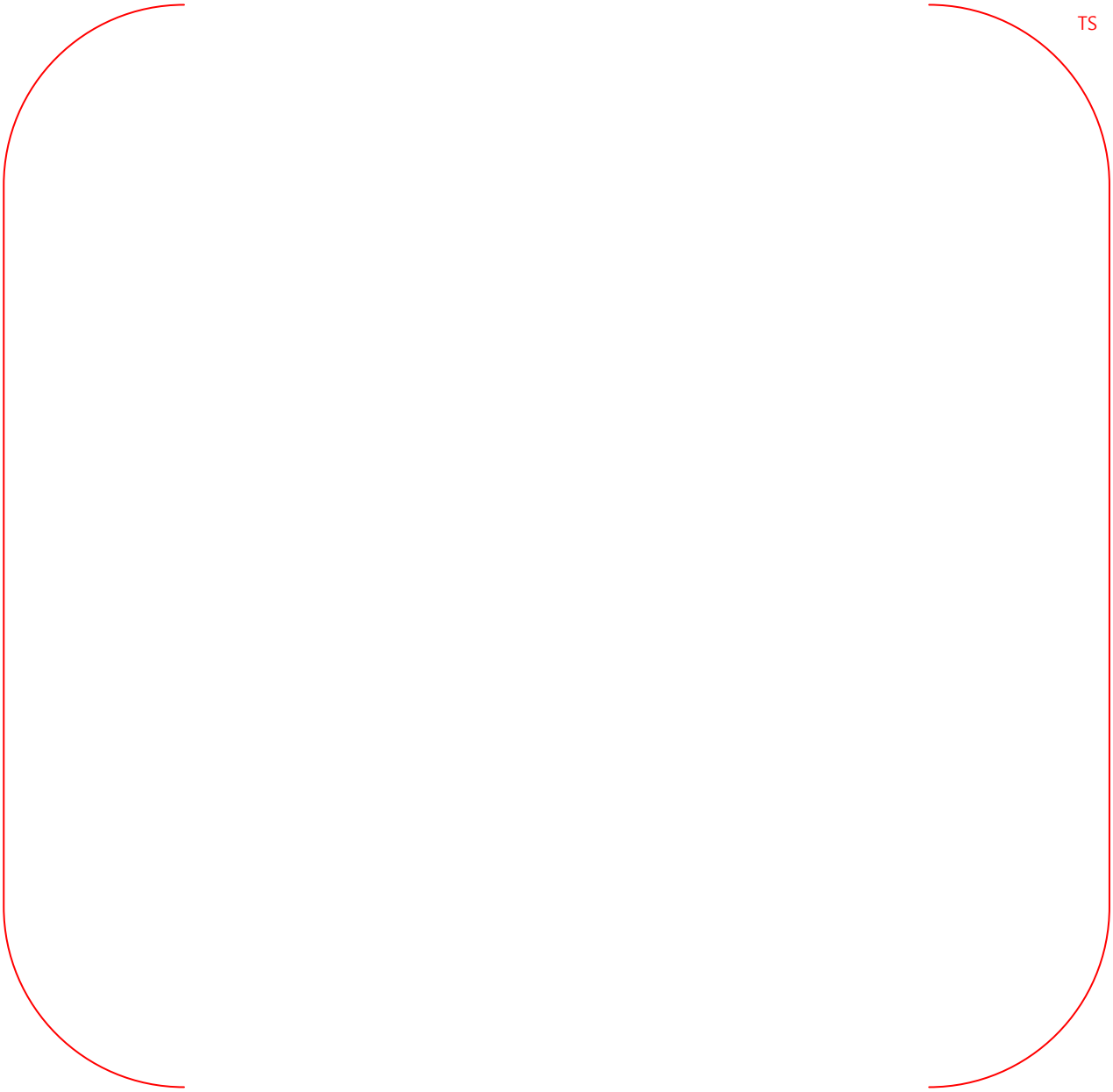

Figure RAI-13-3 Drawing of Discharge Tube of APR1400 SIT-FD

Figure A-4 Drawing of the Exit Nozzle in the Vortex Chamber

Figure A-5 Drawing of the Discharge Pipe connected to the Exit Nozzle

Modify to next page

Figure A-4 Drawing of the Exit Nozzle in the Vortex Chamber

Figure A-5 Drawing of the Discharge Pipe connected to the Exit Nozzle